HELIOPHYSICS II.
ENERGY CONVERSION PROCESSES

edited by
CAROLUS J. SCHRIJVER
Lockheed Martin Advanced Technology Center
and
GEORGE L. SISCOE
Boston University

Contents

2

Observations of solar and stellar eruptions, flares, and jets

by Hugh Hudson

2.1 Introduction

The Sun, regarded as a star, varies on a variety of time scales. These range at least from the 22-year Hale cycle to well below one second. The phenomena associated with the term "solar flare" dominate our thinking about energy conversion from magnetic storage to other forms in the solar corona on time scales below a few minutes. The distinction between a gas dominated by hydrodynamic forces, and a magnetized plasma, becomes extremely obvious in the solar atmosphere and in the solar wind. At first glance we do not need plasma physics to explain the basic (interior) structure of a star; hydrodyamics, nuclear physics, and the theory of radiative transfer seem to do quite well. Nevertheless this apparently simple medium drives the currents that result in the violent and beautiful phenomena we see so readily above its surface. We need plasma physics to describe them.

Understanding the flaring solar atmosphere (photosphere, chromosphere, and corona), since it involves electrodynamics, requires a strong overlap with magnetospheric physics as well as with astronomical techniques useful for studying stellar atmospheres. For many purposes one can accept the standard spherically-symmetric, gravitationally-stratified approximation to the structure of a stellar atmosphere (e.g., Vernazza *et al.*, 1981), but this approach has become obsolete for most problems of current interest. Hansteen (2009) gives a good grounding in modern approaches to the problems involved in physically characterizing the solar atmosphere; see also the lecture notes by Steiner (2007). The new physics being applied to these problems, mainly via numerical techniques, now allows much-improved treatment of three-dimensional structure and time variability, including the study of shock waves. The newest

numerical simulations are now beginning to link the corona to the convection zone self-consistently (e.g., Abbett, 2007).

We begin the chapter with an historical overview, which necessarily follows the development of observational capability. This most important subject is covered in more detail in later chapters of this volume. Solar flares involve the whole depth of the solar atmosphere, and are associated with heliospheric events extending far past the Earth's orbit. Accordingly the observing techniques span the entire range of human capability for classical astronomical remote sensing (see Chapter 12), often with optimization for bright objects, plus the whole range of *in situ* techniques (see Chapter 11). Because solar flares are directly observable only by remote-sensing techniques, there are many important things that we simply cannot know empirically. The results of the observations consist of a sometimes patchy coverage of parameter space, leaving room in the future for many new discoveries even in such a well-observed system (see e.g. Harwit, 1981, and Hudson, 1987, for discussions of how to quantify "discovery" in this respect). This Chapter discusses basic flare phenomena in Section 2.3, analogous astrophysical processes in Section 2.5, and interpretations of the flare observations in terms of large-scale magnetic reconnection scenarios in Section 2.6 as a separate item of great interest.

Confusion often comes from trying to understand these disparate kinds of observation as a whole (e.g., Hudson & Cliver, 2001). To link the pieces of the puzzle together often involves a sketch or cartoon†, and as technology improves it also involves large-scale numerical simulations. The simulations can be used as a kind of forward-fitting tool, with the comparison done in terms of the observations. Often though they are more useful simply as numerical experiments that help to guide the framework of the eventual theory.

The energy release in a solar flare is dominated by particle acceleration, both of electrons (Lin and Hudson, 1976) and of ions (Ramaty *et al.*, 1995; Emslie *et al.*, 2005). This means that the most direct observations are in the X-ray and γ-ray domains; note that non-thermal processes also usually dominate the emission signatures in the radio range (10^7-10^{12} Hz). Please refer to Chapter 11 of this volume for a fuller discussion of the remote-sensing signatures. We will simply comment here that in general the hard X-ray spectrum ($h\nu \gtrsim 10$ keV) is dominated by electrons of this energy or greater, while the soft X-ray spectrum ($h\nu \lesssim 10$ keV) is dominated by the free-bound and bound-bound transitions of a thermal plasma with assumed Maxwellian distribution functions, and also usually assuming $T_e = T_i$. The free-bound process (radiative recombination) may also contribute to the hard X-ray spectrum under certain conditions (Brown and Mallik, 2008).

† See http://solarmuri.ssl.berkeley.edu/~hhudson/cartoons.

2.2 Overview of flare properties

2.2.1 Chronological/chromatic history

Our observational knowledge of the phenomena of solar activity has grown immeasurably since the first flare observation (Carrington, 1859). The development of observational knowledge has of course followed the growth of technical capability. For example, the Carrington flare occurred prior to Röntgen's discovery of X rays or Heaviside's recognition of the ionosphere, and so its "geoffective" significance could not really be assessed.

It is instructive to follow the history of this development (Svestka and Cliver, 1992), which is roughly chromatic (in the sense of new wavebands becoming accessible to observation; see Chapter 12 for more details about technique): the original observations were in white light, done visually through broadband filters. These observations began with Galileo and extended into the 19th century, mainly oriented towards the morphology of sunspots. We now interpret these observations in terms of dynamo theory, a subject beyond the scope of this chapter. Carrington was measuring sunspots when the 1859 flare intruded itself.

Towards the end of the 19th century, spectroscopy and photography improved (e.g., Hale 1930), and the study of solar activity became much richer through access to the chromospheric lines such as Hα. Indeed, flares had been observed spectroscopically by Young, Lockyer, Secchi and presumably others within a decade or so of Carrington's pioneering observation (Svestka and Cliver, 1992). This made it possible to study prominences at the limb, for example, since the spectroscope could suppress the glare of the photosphere and reveal these structures in the corona directly. During this period, a solar flare was a "chromospheric flare," observed by Hα "flare patrol" telescopes around the world. The importance of a flare could be judged from its Hα area (S, 1, 2, 3, where the "S" stands for "subflare") and brightness (F, N, B for "faint," "normal," and "brilliant").

Finally, a third chromatic epoch began in the mid-20th century with the development of radio astronomy (e.g. Hey et al., 1948), and then X-ray (Dellinger, Friedman) and γ-ray astronomy (Peterson, Chupp). Via these techniques the emphasis in solar-flare research has shifted into the corona, where the magnetic energy release results in "loop prominence systems" (a somewhat archaic term referring to Hα arcade structures), closely related to the "sporadic coronal condensations" (a definitely archaic term describing these structures seen in optical coronal emission lines, e.g. from Fe$\textsc{xiv}$). The modern view of these structures is via the soft X-ray monitoring by the GOES and other "operational" spacecraft. We now routinely classify solar flares by their GOES classes: A, B, C, M, and X in decades, with the X class signi-

Table 2.1. *Flare Classifications*

GOES class	1-8Å peak *W/m*^{2}	Hα class	Hα Area *Millionths of disk*	CME rate[a] *percent*	Events/year *max/min*
A	$>10^{-7}$	-	-	-	-
B	$>10^{-6}$	S	<200	-	-
C	$>10^{-6}$	1	>200	20	>2000/300
M	$>10^{-5}$	2	>500	50	300/20
X	$>10^{-4}$	3	>1200	90	10/one?
-	$>10^{-3}$	4	>1200	100	few?/none?

[a]Yashiro et al. (2005) (approximate values)

fying 1-8Å energy fluxes greater than 10^{-4} W/m^2, on the order of 0.01% of the solar luminosity. Table 2.2.1 summarizes these and other properties, with very approximate correspondences between the Hα and GOES X-ray systems, and very approximate ranges for the number of flares that occur each year at maximum and minimum of the solar cycle.

These stages in the development of observational capability have essentially changed the meaning of the word "flare," for example. Hale used the term "eruption" and recent decades have seen some confusion about nomenclature (Cliver, 1995). We now know that the physics of a flare, or other form of solar activity, requires rapid restructuring of the coronal magnetic field where energy has been built up much more gradually. In summary, the chronological/chromatic history of solar flare research has generally proceeded through visible light (the photosphere), spectroscopy of the chromosphere, and finally X-rays and radio waves (the corona). At present it appears that the most important region physically is the chromosphere again (e.g. Hudson 2007a), because it mediates the dramatic changes of state between the photospheric and coronal plasmas.

2.2.2 Flare phases

The release of energy can either be "impulsive" (Kane and Anderson, 1970), with time scales sometimes faster than 1 s, or "gradual." The impulsive and gradual signatures of a flare extend across the entire electromagnetic spectrum in a complicated way, as illustrated in Figure 2.1. The terminology may not seem appropriate when one considers a slowly developing flare-like event, such as a quiet-Sun filament eruption (Harvey *et al.*, 1986; Hudson *et al.*, 1995a); in such a case the "impulsive phase" may take tens of minutes to evolve, and the

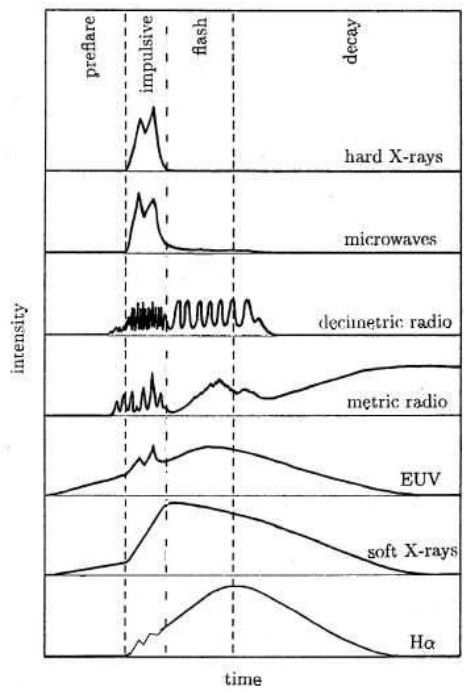

Fig. 2.1. Schematic view of the time histories of flare emissions in different wavelengths, showing the intermingling of impulsive-phase and gradual-phase signatures across the spectrum (from Benz, 2002). Note the wide variety of radio signatures.

hard X-ray emission may be below the detection level. Thus we don't know how "impulsive" the energy release really is in such an event, but in other respects it has the morphology of an ordinary active-region flare.

We understand the impulsive and gradual phases to show the main energy release and its aftermath (secondary effects), with the proviso that it is really not just that simple. The most prominent "aftermath" is the action of coronal magnetic loops as an energy reservoir, with cooling time scales that can approach hours. This reservoir function is often described as the "Neupert effect" (Neupert, 1968 Dennis and Zarro, 1993): the coronal manifestations of a flare tend to lag behind its chromospheric ones. This results from the finite time scale associated with the coronal density increase during the impulsive phase, via the process of "chromospheric evaporation." The decay time scale reflects its slower cooling and return to the lower atmosphere. The new material in the corona could be seen in the coronal emission lines (e.g. Billings, 1966), via free-free emission at radio wavelengths (e.g., Kundu, 1965), or via free-free emission at soft X-ray wavelengths (e.g., Hudson and Ohki, 1972). This "evaporation" process caused confusion from the outset, to the extent that the

coronal material of the gradual phase of a flare could best be seen, prior to the advent of the new techniques, as a "loop prominence system" in Hα. Such a "prominence," which results from the cooling of plasma even hotter than the ambient corona, physically has nothing to do with a true solar prominence. An *Hα filament* (when seen on the disk) or a *quiescent prominence* (when seen above the limb) is a relatively stable inclusion of cold plasma in the corona.

The different atmospheric layers have a high degree of interconnectedness. Since a flare marks a transition between one quasi-stable configuration and another, the ordinary law of hydrostatic equilibrium dictates the run of pressure up through the atmosphere. A flare increases the gas pressure in the corona, at the expense of magnetic energy, and this can readily be detected at all levels (e.g., Machado et al. 1975). The hydrostatic scale height for pressure is given by $2k_BT_e/mg_\odot$, where k_B is the Boltzmann constant, T_e the temperature, and m the mean molecular weight. For a flare temperature of 10^7 K, this scale height is a large fraction of the solar radius, much larger than the flare loop structures. Thus the vertical structure is isobaric in the upper chromospheric and coronal regions, and the chromosphere acts as a reservoir of mass to maintain this isobaric state as the flare loops cool and lose pressure quasi-statically.

2.2.3 Flare antecedents

The physical condition of the corona prior to a flare must contain the information one needs to predict its occurrence. Many flares, as seen in GOES soft X-ray or microwave light curves, have a pre-event increase, mainly seen in free-free (bremsstrahlung) continuum. This can be unambiguously identified with an increase of the emission measure ($\int n_e^2 dV$) of hot plasma in the corona. But is such a precursor physically related to the flare that is going to happen? Is it indirectly related, or is it a coincidence made more likely by frequent flare occurrence in a given active region? These questions are convolved with appearance of flickering, swelling, rising, and other signs of activity in a filament that is about to erupt (e.g., Crockett *et al.*, 1977; Webb, 1985; Gaizauskas, 1989; Fárník *et al.*, 2003; Chifor *et al.*, 2007). The appealing picture of "tether-cutting" (Moore and Labonte, 1980) makes sense in such a context.

Sometimes there is virtually no early activity and so it is difficult to accept this as a prerequisite for flare occurrence. The bright flare loops themselves usually appear at new locations as identified by their "line-tied" footpoint locations (Fárník *et al.*, 1996; Fárník and Savy, 1998; Hudson *et al.*, 2008). In such cases we must assume that the magnetic flux tubes anchored at the same footpoints as the flaring loops were empty and dark prior to the flare.

In the lower solar atmosphere, and especially in the magnetograph and chromospheric observations, there are patterns that anticipate flare occurrence (e.g., Rust et al., 1994; Schrijver, 2007). Zirin & Liggett (1987) found an almost one-to-one correspondence between the "delta spot" sunspot configuration and the occurrence of X-class flares. The most important of these is "flux emergence," revealed in Hα as an "arch filament system" or simply as an "emerging flux region" (e.g. Vorpahl, 1973; Nitta & Hudson, 1998). We can interpret this as one of the ways in which the coronal field can be stressed, i.e. to carry field-aligned currents, for the duration of the energy build-up that precedes the flare itself. The time scale for this build-up and release – not yet observed as a true relaxation oscillator – appears to be a few hours.

2.2.4 Flare types

For the most part solar flares have similar properties, and their extensive parameters tend to scale together in a systematic way. This is one view of the "big flare syndrome" (Kahler, 1982). This suggests that all flares fit one pattern, and that the energy release is just a matter of energy scale. Pallavicini et al. (1977) identified two types of solar flare, which we refer to as "confined" and "eruptive" here. No solar property appears to have a bimodal distribution that clearly distinguishes these two categories, and so this classification remains somewhat arbitrary. However in the domain of solar energetic particles (SEPs) there is a bimodal separation into "impulsive" and "gradual" events, (e.g., Reames, 1999). The names given to these categories may not exactly match the observed properties. Extremely impulsive flares may certainly be eruptive as well (e.g. Nitta and Hudson, 2001). The extensive properties of flares (for example, CME kinetic energy and soft X-ray peak brightness; see Section 2.3.5, but there are many other examples) generally correlate over 4-5 decades with an rms scatter of about a factor of two. This means that the dynamics of the solar atmosphere during a disruption follows some regulated development that generally ignores the distinction between confined and eruptive properties. We do not yet have theories or numerical simulations that are sufficiently model-independent to explain this broad regulation of flare properties.

2.2.5 Flare-microflare occurrence patterns

The frequency distribution of flare energies has a featureless power-law distribution $dN/dE \propto E^{-\alpha}$ (Akabane, 1956; Drake, 1971; Crosby *et al.*, 1993). This distribution extends over several decades of energy, from the domain of major flares with energy of order 10^{32} ergs down to the "microflare" domain around

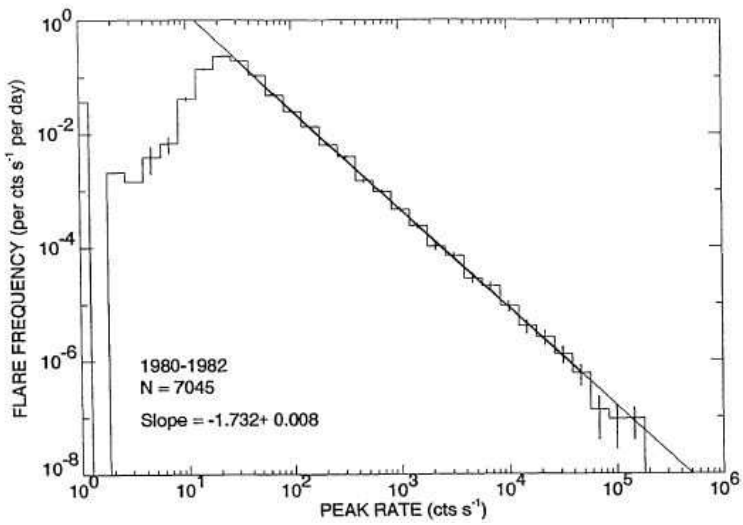

Fig. 2.2. Distribution of peak counting rates of 7,045 hard X-ray bursts observed over 1980-1982 by the HXRBS instrument on board the Solar Maximum Mission (Crosby et al., 1993). Note the fidelity of the power law, down to a low-rate rolloff due to selection effects; also note the lack of a high-rate rolloff in this range of observations.

10^{26} ergs. Many extensive parameters associated with solar flares show this kind of power-law distribution, which implies scale invariance. This property probably has an important physical significance, but it is deceptive: *average* properties of such distributions only reflect the sensitivity of the observation, not anything physically significant.

The slope of the flare-microflare power law ($\alpha < 2$) suggests that the microflares do not contribute in a dominant manner to the total energy in flaring; indeed, the flare-microflare occurrence distribution must steepen above some total energy in order not to diverge in total energy (Hudson, 2007b). Figure 2.2 shows a distribution of hard X-ray peak fluxes, taken here to serve as a proxy for total flare energy. Crosby et al. find a power-law index of $\alpha = 1.732 \pm 0.008$ for this sample, in good agreement with Akabane's original estimate of $\sim$1.8 using peak microwave fluxes. It appears that the peak flux of the burst, whatever the wavelength, may scale in a similar way with the total event energy. This is consistent with the "big flare syndrome" scaling of extensive parameters noted in Section 2.2.4.

Physically, the microflares look like less-energetic versions of major flares (e.g. Christe et al., 2008; Hannah et al., 2008). However, at least two clear distinctions do appear as one goes along the distribution of flare magnitudes. First, the major flares tend to have a strong association with CMEs. This becomes almost one-to-one for X-class GOES ratings (e.g., Yashiro *et al.*,

2005; see Table 2.2.1). Second, the minor events tend to have more clearly recognizable soft X-ray jets (e.g., Shimojo *et al.*, 1996; see the illustration in Figure 2.5). There may be a tendency for arcades to form in more energetic events, as compared with the more common appearance of a single dominant coronal loop in a less-energetic event.

2.3 The basic phenomena of a solar flare

In the photospheric spectrum we see solar flares as brief flashes of white light and UV continuum. At present these sources are often not resolved either in space (arcsec scales) or time (few sec scales) (Hudson *et al.*, 2006). The bright emission regions are embedded in the "ribbon" regions that become more prominent in the chromospheric lines. In the coronal emissions one sees bright coronal loops developing slowly, with those from the highest temperatures appearing first and then cooling down through generally longer wavelengths, while at the same time shrinking in length (Švestka et al., 1987).

In the following sections we outline the basic phenomena of a flare, including the development of a coronal mass ejection (CME). More energetic flares almost always have this association, whereas weaker flare events usually do not. The exception to this rule is the major CME events that come from quiet-Sun filaments, for example the "polar crown" filaments at latitudes well above those of the sunspot regions. Such events may have spectacular CMEs but only barely detectable large-scale chromospheric/soft X-ray signatures (Harvey *et al.*, 1986). Furthermore the soft X-ray jets discovered with *Yohkoh* (Shibata *et al.*, 1992; Strong *et al.*, 1992) invariably are associated with *microflares*, discussed separately below. These are less-energetic events. The jets are essentially plasma motions parallel to the magnetic field, whereas the more energetic flares associate better with CMEs, which have the appearance of loop expansion and hence perpendicular plasma motion. Note that these perpendicular plasma motions usually begin in active regions where the plasma β (ratio of gas pressure to magnetic pressure) is low (see Gary, 1989, for a review of coronal β values). Microflares, flares, and CME-related major flares all look similar in many respects, except for scale, but the major CME-related flares tend to have the LDE ("long-decay event" or "long-duration event") characteristic of long-lived arcade sources, as discussed below in Section 2.3.3.

2.3.1 Flare luminosity and mechanical energy

Solar flares are not luminous on the scale of the total solar irradiance ("solar constant"), although they may produce a localized brightening seen against the bright photosphere. The powerful flare of November 4, 2003 was the first

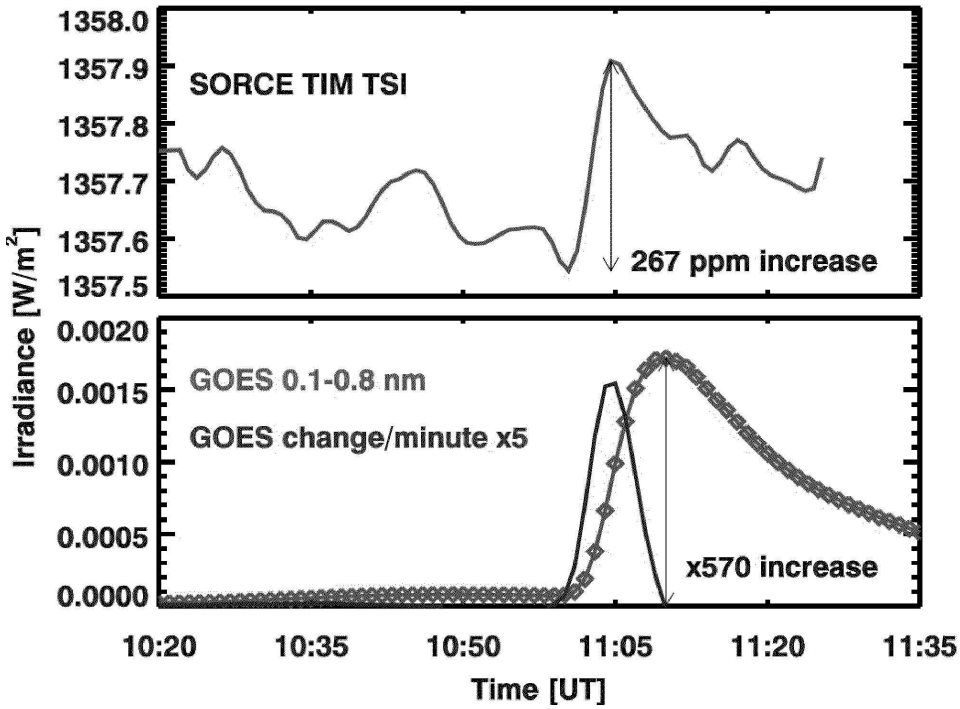

Fig. 2.3. *Upper:* SORCE observations of total solar irradiance variations during the major flare of 2003 November 4 (Woods et al., 2006). *Lower:* the simultaneous time history from GOES soft X-rays, with the smooth black line showing the time derivative as a guide to the impulsive phase, assuming the Neupert effect.

that could actually be detected in the total solar irradiance, by the radiometer on board the SORCE spacecraft (Woods *et al.*, 2006) as shown in Figure 2.3. The signal, a roughly 5σ significance, amounted to about 300 ppm of the total signal, or 0.3 millimagnitudes in astronomical terms. There is a solar background noise level for such a measurement due to convection and oscillations; this amounts to some 50-100 ppm spread out over bandwidth of a few mHz (e.g., Hudson, 1988).

The localized brightening of a flare is much easier to see, of course, via an image even in white light. Carrington described his 1859 discovery as resembling the brilliance of Vega (α Lyrae), for example. Although it has been difficult to obtain comprehensive photometric observations across the entire spectrum of a flare, we now know enough about the energy distribution to know that what Carrington saw was a major fraction of the flare luminosity (see Figure 2.3). Soft X-ray emission, for example, contains only 5-10% as much luminosity. This gradual component, as discussed below, results from a

thermal distribution (hot gas) for which the X-ray emission itself is a dominant cooling term. The non-thermal tail of the X-ray spectrum ($h\nu > 10$ keV), on the other hand, is due to bremsstrahlung from stopping particles. The bremsstrahlung mechanism is very inefficient, providing a fraction of order 10^{-5} of the energy losses. The rest of the energy winds up in longer-wavelength radiation, notably the white-light continuum (Hudson, 1972; Fletcher *et al.*, 2007).

We must also consider the bulk kinetic aspects of flare luminosity, since for major events a CME almost invariably results. CME kinetic energies can rival flare luminosities (e.g., Emslie *et al.*, 2005) in such cases. In rare cases a CME can occur in the absence of a major perturbation of the lower atmosphere. The most unambiguous example of such an occurrence was discussed by Webb et al. (1998). The partition of energy in a flare/CME event remains unclear physically and hard to determine observationally.

2.3.2 The impulsive phase (hard X-rays, footpoints)

The impulsive phase of a flare marks the period of intense energy release and strong non-thermal effects, including the launching of the CME. The traditional observational tools for the impulsive phase are hard X-ray emission and gyrosynchrotron emission at cm to mm radio wavelengths. The hard X-rays normally show two dominant footpoints embedded in ribbon regions of opposite magnetic polarity, but we do not presently understand why there are normally just two. The sources are compact and rapidly variable, and we associate them with the UV and white-light continuum emissions that also come from the footpoint regions, as illustrated in Figure 2.4. Other wavelengths (see Figure 2.1) show impulsive emission components as well as gradual ones. A clear impulsive-phase signature also appears even in the total irradiance, as shown in Figure 2.3, but rarely, because it requires the most energetic of events.

The hard X-ray spectrum above about 10 keV plays a central role in our understanding of the impulsive phase because the collisional energy losses of the bremsstrahlung-emitting electrons rival the total flare energy itself. This relationship can be established directly by inverting the hard X-ray spectrum, under model assumptions. The "collisional thick target model" (Kane and Donnelly, 1971; Brown, 1971; Hudson, 1972) envisions a black-box accelerator of 10-100 keV electrons in the corona, with a directed beam penetrating to the chromosphere or even photosphere to excite UV and white-light emission. This simple model has become less tenable as spatial resolution improves, since the WL/UV brightenings seen by TRACE imply beams with extreme intensity (Hudson *et al.*, 2006; Fletcher *et al.*, 2007).

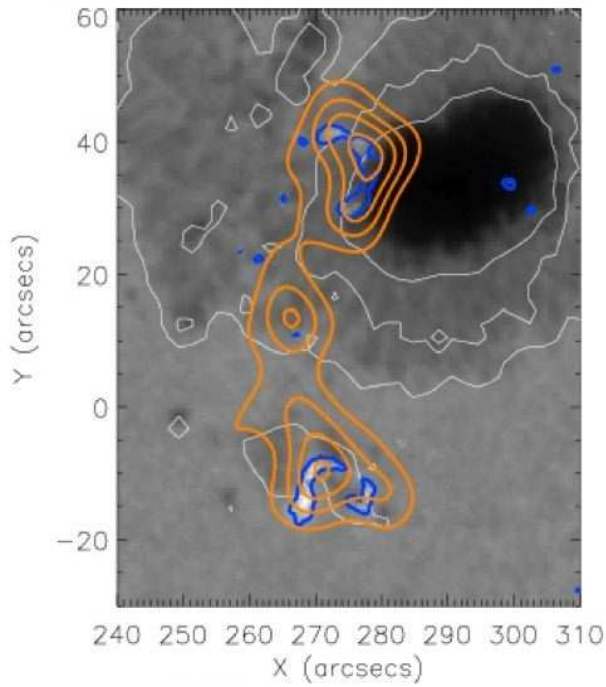

Fig. 2.4. TRACE white light (blue contours) and RHESSI hard X-ray (red contours; 25-50 keV) observations of a flare of 2002 July 24 (Fletcher et al., 2007). Note the extremely compact (arc sec), and temporally unresolved (∼10 s), white-light patches in the north and south footpoint regions. The RHESSI source in between the footpoint regions is not associated with the white-light emission.

The impulsive phase also corresponds to global processes, even though the radiated energy comes from exceedingly compact sources. These include coronal dimmings and CMEs, which we discuss separately in Section 2.3.5. In addition, there is the appearance of an "implosion," as suggested by Hudson (1972) and possibly now observed in RHESSI and other data (Sui and Holman, 2003; Veronig *et al.*, 2006). The implosion results from the reduction of magnetic pressure via the energy conversion, which the volume of the field. The characteristic inward motions could represent flows associated with Poynting flux as the magnetic equilibrium changes (Emslie and Sturrock, 1982; Melrose, 1992).

2.3.3 The gradual phase (soft X-rays, ribbons)

"Gradual phase" refers to the thermal emission of the hot coronal material evaporated during the impulsive phase, plus the strong transition-region and chromospheric emissions driven by the cooling of these coronal loops. The

loops connecting the roughly parallel ribbons form a cylindrical *arcade* structure, divided into many unresolved loops. These hot X-ray and EUV loop structures were first seen in early optical observations of coronal forbidden lines. The loops were also termed *sporadic coronal condensations* (e.g., Billings 1966). The hot regions eventually cool to form the Hα loop prominence system, whence thermal instability leads to the phenomenon of "coronal rain". The cooling also corresponds to shrinkage, as the gas pressure diminishes; shrinkage may also relate to the gradual release of energy as the coronal equilibrium returns to a stable configuration (Švestka *et al.*, 1987; Forbes and Acton, 1996). This is the process termed "dipolarization" in the geoagnetic community and basically resembles the impulsive-phase implosion noted above.

2.3.4 Jets (parallel motions)

Soft X-ray jets were discovered with the *Yohkoh* soft X-ray telescope (Shibata *et al.*, 1992; Strong *et al.*, 1992; Shimojo *et al.*, 1996). They found an immediate interpretation in terms of the emerging-flux reconnection scenario (Heyvaerts *et al.*, 1977). The jet material is hot plasma projected along magnetic flux tubes that may open out into the heliosphere, or in some cases close on large scales before entering the solar wind. These are plasma flows parallel to the apparent field direction. The jet sources have a strong association with radio type III bursts – known to come from nonthermal electrons streaming outwards along open flux tubes (Aurass *et al.*, 1994; Kundu *et al.*, 1995) – and also with electron events observed in interplanetary space (Lin, 1974; Krucker *et al.*, 2007; see also Nakajima and Yokoyama, 2002). Invariably a compact flare appears near the jet's point of origin near the chromosphere (Shimojo *et al.*, 1996).

The jet-associated microflares have magnetic connectivity that permits access to the heliosphere, and they have other occurrence patterns linking them to emerging (or disappearing) magnetic flux (Shimojo *et al.*, 1998). The jet-associated microflares seem to be compact and less energetic flares, and *Hinode* observations clearly show then to be part of a continuum of weaker and weaker jet-like events (Shibata *et al.*, 2007) found in the quiet Sun and especially visible in the polar regions (Figure 2.5). Soft X-ray jet structures are seldom as visible in major flares.

2.3.5 Coronal mass ejections (perpendicular motions)

Major flare events almost invariably involve the "opening" of the magnetic field as a CME (e.g. Hundhausen et al. 1994); see Table 2.2.1 for the statistics. This involves the unstable expansion of the field (equivalent to a motion

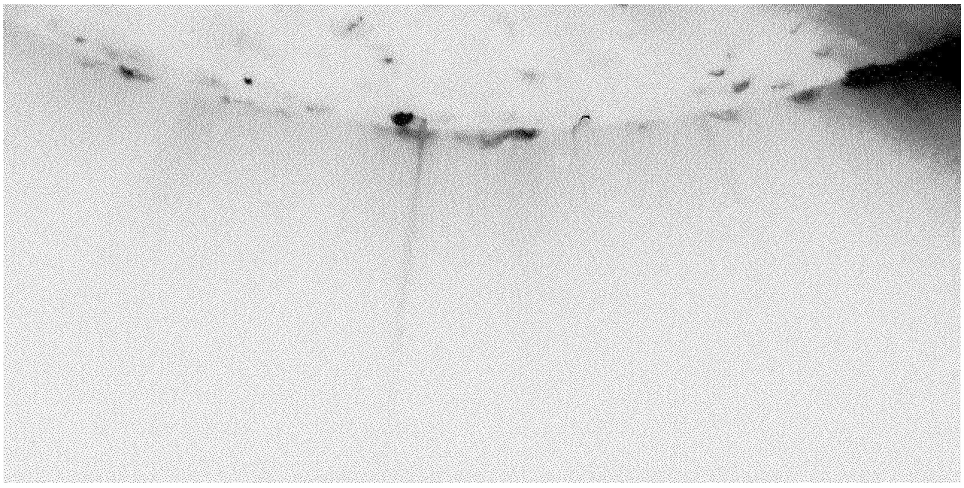

Fig. 2.5. Soft X-ray image of the south polar region, with an inverted color table, showing a highly collimated polar jet structure (Courtesy P. Grigis). Note that this is a coronal-hole jet, but that similar features often occur in active regions in association with microflares (see Section 2.2.5).

perpendicular to the field). Note that at low plasma β, the gas whose emission we observe (the mass of the CME) has little influence on the dynamics. Observationally, in the Thomson-scattering brightness measurements made by a coronagraph, we often see the classic three-part structure: front, cavity, and filament (Figure 2.6 and e.g. Hundhausen, 1999). This pattern makes it clear that the CME originated in a filament cavity near the surface of the Sun. A filament cavity (see e.g. Engvold, 1989, but note that there seems to be no recent review of this important subject) consists of long, basically horizontal field, presumably more intense than its overlying "tie-down" more potential field (Gibson and Fan, 2006; Martin *et al.*, 2008; Schrijver *et al.*, 2008).

The interpretation of the front structure of a CME is complicated. One expects, from the standard models (see Chapter 3) that this would incorporate coronal material contained in the overlying magnetic flux tubes as they are expelled from the corona and become "open." There should also be a sweeping-up of ambient coronal or solar-wind material, and we would expect the occurrence of a bow wave analogous to that of the Earth in the solar-wind flow. The presence of such a bow wave is consistent with observations of type II radio signatures at hectometric-kilometric wavelengths. The emission from these bursts requires the shock condition to have been met (e.g. Kundu, 1965), and their velocities are consistent with the known outward velocities of the CMEs that provide the driver gas for this large-scale shock. To clinch the picture, we also observe the shock when it impacts the magnetosphere with

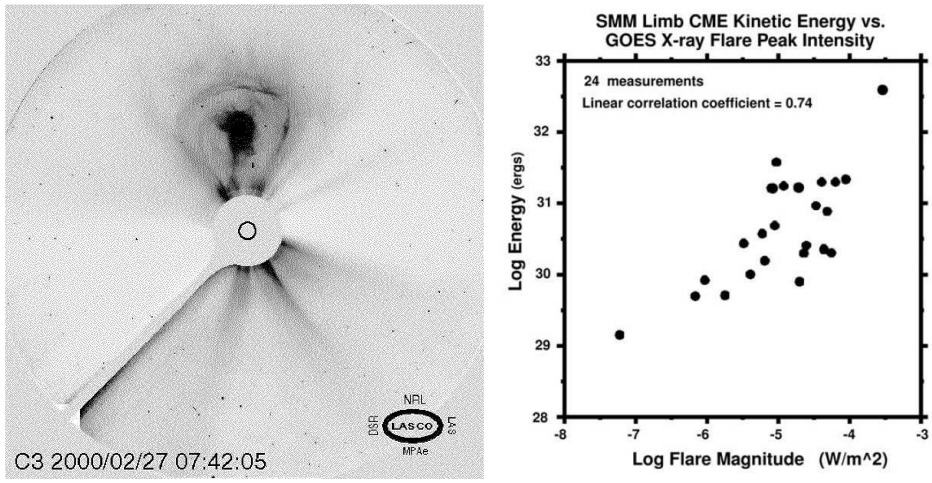

Fig. 2.6. *Left:* Coronagraph observation of a CME that nicely shows the three-part structure: front, cavity, and (the bright core) filament (this is a file image taken from the LASCO database, presented in a reverse color table)). *Right:* Correlation between inferred CME kinetic energy and peak GOES soft X-ray flux (Burkepile et al., 2004).

the classic Storm Sudden Commencement (SSC) signature (e.g., Chapman & Bartels, 1940).

The mass of a CME largely comes from below the occulting edge of the LASCO C2 coronagraph. Indeed, a glance at LASCO movies readily available on the Web† shows mass flow long after the three-part structure has vanished. This late flow certainly originated in the lowest corona or even chromosphere.

Modern images in coronal emissions such as soft X-rays allowed a comparison of the coronal state before and after a CME event. Such comparisons revealed "dimmings," readily interpreted as the evacuation of the mass of the corona by the CME eruption (Hudson *et al.*, 1995b; see also Rust, 1979, for the earlier *Skylab* observation). The soft X-ray dimmings presumably correspond to the coronal depletions found via similar before/after comparisons of the visible corona. (Hansen *et al.*, 1974)

2.3.6 Global waves (coronal and other)

There are at least five types of large-scale wave structures associated with solar flares and CMEs, perhaps not all distinct: helioseismic, metric type II, Moreton, interplanetary type II, and EIT. The Moreton waves (Athay and Moreton, 1961) can now be detected at several different wavelengths. Originally discovered in Hα (the chromosphere), they are fast (of order 1,000 km/s)

† http://sohowww.nascom.nasa.gov/data/data.html

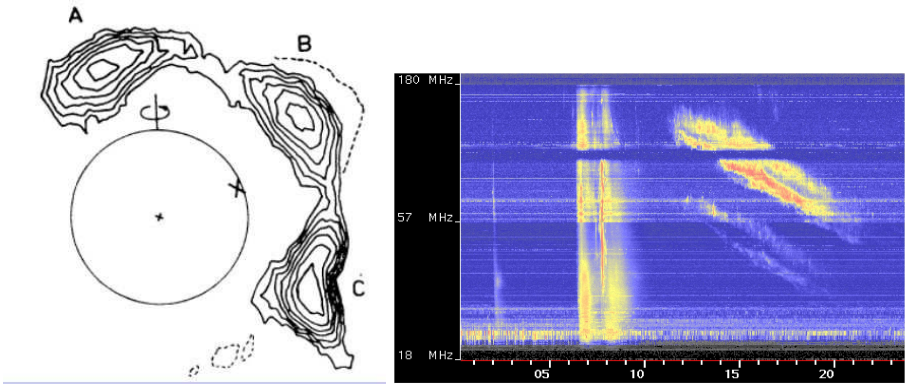

Fig. 2.7. *Left:* Culgoora image of a type II burst associated with a major flare (Palmer & Smerd, 1972). Note how this plasma-frequency radiation appears to wrap around a concentric spherical surface, presumably at the right mean density. *Right:* Radio spectrogram (frequency vs time) of a different major flare, illustrating type III bursts (fast drift, produced by streams of energetic electrons) and a type II burst (slow drift, fundamental/harmonic structure produced during the propagation of a large-scale shock wave), also from Culgoora.

waves radiating, normally into restricted sectors, from the flare site. The standard theory of Uchida (1974) describes these chromospheric waves as the skirts of global fast-mode shock waves actually propagating in the corona; the wave energy refracts into the chromosphere because of its lower Alfvén speed.

Large-scale coronal shock waves had long been known from meter-wave radio astronomy, where the radio signatures clearly imply that the shock condition has been met (Wild *et al.*, 1963). The type II burst (Figure 2.7) is relatively rare, and it is observed best at the frequencies below ∼200 MHz. As with the "fast-drift" type III bursts, the assumption of emission at the local plasma frequency (or its harmonic) allows for a height estimation by assuming a coronal density model. The derived motions point to an origin in the impulsive phase of the flare, but this requires an extrapolation because of the shock "ignition" requirement (Vršnak and Lulić, 2000). We also know directly of *interplanetary* shock waves driven by CMEs as bow waves, both from longer-wavelength radio astronomy and also from the *in situ* observations (and the SSC response of the Earth's magnetosphere to the impulse).

The EUV observations from SOHO disclosed a remarkably rich pattern of "EIT waves" (Moses *et al.*, 1997; Thompson *et al.*, 1999). The EUV signature is somewhat complicated, and it appears that multiple causes can produce wave-like disturbances (Biesecker *et al.*, 2002), including the classical Moreton wave.

Finally, the helioseismic waves discovered by Kosovichev & Zharkova (1998)

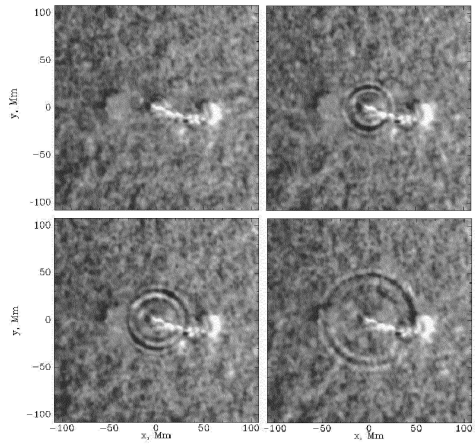

Fig. 2.8. The original helioseismic wave observed from the singular solar-minimum flare of 1996 July 7 (Kosovichev & Zharkova, 1998), from the "last best active region" of that solar cycle (Hudson et al., 1995). The figure shows an amplified wave via Doppler images, with the wave representation based on the observed Fourier components. More recent helioseismic waves are directly visible in the filtered images.

seemed rare at first, but now there are several examples. Figure 2.8 shows the original event, that of 1996 July 9. These waves result from energy coupled into the interior by the flare process. The excitation of such a wave is thus closely associated with the dynamics of the deepest atmospheric layers that we can see into. This probably involves the most energetic aspects of a flare. In this context we note the 1.56μ "opacity minimum" observations of Xu et al. (2004) and also the γ-ray observations of Share et al. (2004; see also Schrijver et al., 2006 for further discussion).

2.3.7 Magnetic signatures

The observation and interpretation of solar magnetic signatures has improved dramatically in the past decade, with new facilities such as the ground-based SOLIS and *Hinode* satellite providing vector Zeeman measurements, for example. Such measurements show clear flare-associated permanent (stepwise) changes (Kosovichev and Zharkova, 1999; Wang *et al.*, 2002; Sudol and Harvey, 2005), which would be expected if the stresses in the coronal field had their origins in motions below the photosphere ("energy build-up"). In addition there are vigorous activities related to interpreting the data in terms of the coronal field, which is almost unobservable (but see Lin *et al.*, 2000; Tomczyk *et al.*, 2008) and in any case is optically thin. The extrapolations have an

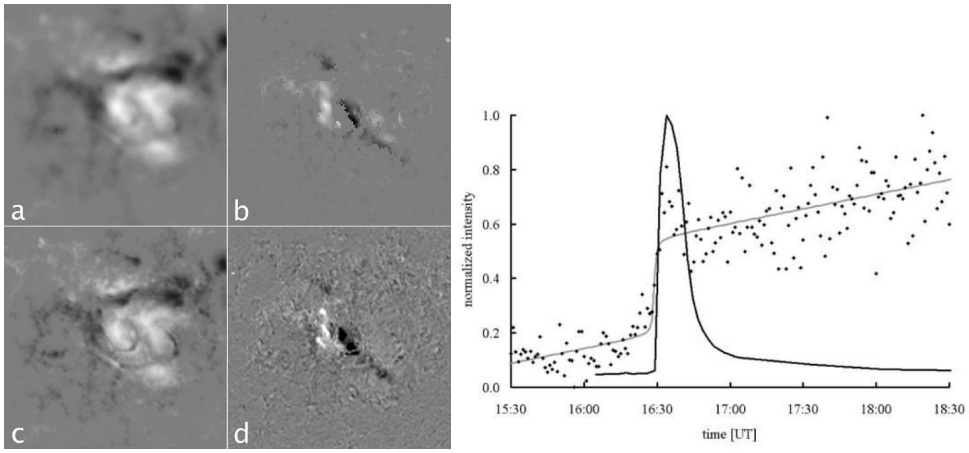

Fig. 2.9. *Left:* Map of the stepwise photospheric field changes in the flare of 2003 October 29. Panels (a) and (c) show the GONG and MDI magnetograms; panels (b) and (d) show their before/after changes, respectively. *Right:* Time variations for the flare of 2001 August 25, showing the GOES light curve as a smooth line and the GONG data as points. The fluctuations are large and there is a background trend, as in many events, but the stepwise change is clear. It (typically) coincides with the impulsive phase of the flare. Both illustrations taken from Sudol & Harvey (2005).

excellent chance to be extremely informative in active regions in particular, since the active-region corona has low plasma β values.

Figure 2.9 (left) shows the stepwise magnetic changes derived by Sudol & Harvey (2005) for the X10 flare of 2003 October 29. These are well-defined and appear to delineate the general regions of the flare ribbons, and within the time resolution of the data they tend to happen in coincidence with the impulsive phase of the flare. There is thus no reason not to associate these changes with the source of flare energy. Liu et al. (2005) report similar changes and show how one could interpret them in terms of simple global changes in the coronal field (Hudson, 2000).

The implications of these new developments are clear: when we can do the same thing with vector fields, and in addition do the measurement well above the photosphere, we will be able to reconstruct the before/after 3D field structure in an active region and learn quite directly about the exact geometry of the instability. The measurement of the chromospheric field, as opposed to that of the photosphere which is not force-free, is important to minimize the effects of stresses imposed by photospheric flows. Note that future "frequency-agile" imaging spectroscopy in the microwave band offers a precise and complementary way of checking the observations and extrapolations (White, 2005), since this wavelength range includes the electron cyclotron (Larmor) frequency of

these fields. Until the advent of these new capabilities, it is unlikely that a quantitative understanding of the actual field restructuring will be possible.

2.3.8 Coronal nonthermal events

Prior to *Yohkoh* and RHESSI, meter-wave radio astronoomy was the main source of knowledge about non-thermal processes in the corona (e.g., shock waves and particle acceleration). The radio observations are very sensitive and result from interesting physical processes (see Kundu, 1965, for much interesting detail, or Bastian et al., 1998, for a more recent review of radio techniques). The type II bursts, for example, involve many small-scale accelerations of ambient electrons to few-keV energies (the "herringbone" structure). However the meter-wave have low angular resolution and the emission mechanisms (except for the free-free mechanism) have complicated dependences on the physical parameters of the emitting region and its environment. Thus it would be extremely valuable to detect some of these sources in X-radiation, which is more direct.

Krucker et al. (2008) review the current observational status of coronal hard X-ray observations. As more sensitive data become available, it is clear that the corona is a rich source of hard X-ray emission, as expected, but the details are in some cases unexpected. For example, one would confidently expect that the electron streams commonly observed at one AU (Lin, 1974) would produce at least thin-target bremsstrahlung near their point of acceleration in the corona (Lin and Hudson, 1971). We still do not have clear observations of this emission (Krucker *et al.*, 2007). On the other hand, coronal hard X-rays associated with CME eruptions appear to be common (Krucker *et al.*, 2008), and these may be related in some manner to the radio type IV bursts. Type II burst sources can be observed in soft X-rays (Khan and Aurass, 2002; Hudson *et al.*, 2003), but not yet in hard X-rays (the signature of the nonthermal particles) because of lack of sensitivity.

One of the most striking of the new RHESSI coronal hard X-ray sources is shown in Figure 2.10 (Krucker *et al.*, 2008). The high energy of observation (250-500 keV shown in the figure) means that the source electons were relativistic. Footpoint sources appeared early in the event, but the coronal source remained bright and decayed in flux with a nearly exponential decay with a time constant of about 5 minutes, similar to that observed in the prototype coronal hard X-ray event of 1969 March 31 described by Frost & Dennis (1971).

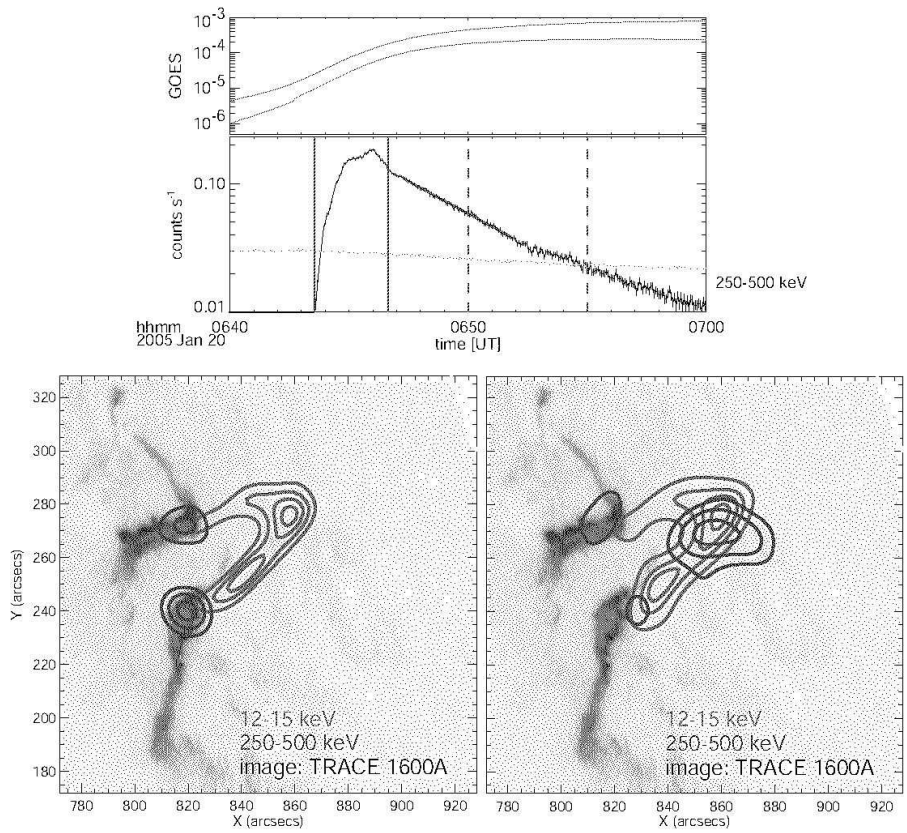

Fig. 2.10. Hard X-ray sources from the 2005 January 20 event. *Upper:* GOES and RHESSI light curves. *Lower:* Early image showing well-developed footpoints at 250-500 keV (dark contours), and a later image showing the persistent coronal hard X-ray coronal source. The light contours show large-scale loop structures with thermal spectra.

2.4 Flare Energetics

2.4.1 Magnetic energy storage

An active region with large sunspots creates a localized region of strong magnetism in the corona. The basic potential-field description of the sunspot fields already predicts strong fields at altitudes comparable to the spot diameter, and in fact microwave observations do show such fields (e.g., Brosius and White, 2006). Extreme values of the Alfvén speed and plasma β could result; for $|\mathbf{B}| = 10^3$ G and $n_e = 10^8$ cm^{-3} at a height 10^9 cm above a large sunspot umbra, for example, one would find $v_A = 0.7$ c and $\beta = 7 \times 10^{-6}$ (for T = 10^6 K).

Energy storage in excess of the basic potential-field minimum, which cannot be converted into other forms, comes from currents injected into the corona

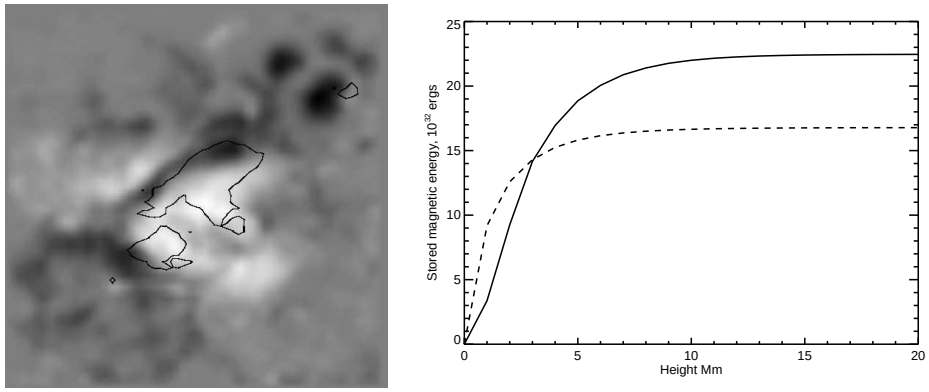

Fig. 2.11. The stored magnetic energy in a nonlinear force-free field extrapolation for AR 10486 computed by J. McTiernan using the technique of Wheatland et al. (2000). *Left:* The B_z component of a chromospheric vector magnetogram for AR 10486, 2004 October 29 18:46 UT. The contour shows the 50% level of the excess over the energy content of the corresponding potential field, at an altitude of 6 Mm. *Right:* Increase of total energy with height in the data cube of the extrapolation (dimension $65 \times 4''$). The dashed and solid lines show the potential and non-potential integral energies, respectively. The 50% level gives a rough idea about the location of stored magnetic energy; it is higher for the non-potential field but still located close to the base of the corona.

from below the photosphere. These currents intensify and enlarge the active-region field, and the restructuring of the currents and field can release flare energy. Figure 2.11 shows an estimate of the stored magnetic energy in active region 10486, which produced the flare with the bolometric excess shown in Figure 2.3. Note that the excess magnetic energy, using the non-linear force-free model of Wheatland et al. (2000), apparently can actually exceed the potential-field energy even though strongly twisted coronal structures are not often seen.

2.4.2 Partition of energy release

The energy released from its magnetic storage is lost to the corona either as radiation or in the form of mass motions. Note that thermal conduction should generally lead to excess radiation at transition-region or chromospheric temperatures (e.g., Emslie *et al.*, 2005). The initial energy release is dominated by the acceleration of high-energy particles (Lin and Hudson, 1976), which are relatively easy to detect from their hard X-ray, γ-ray, and radio signatures. There is also presumably some direct heating in the sense of Ohmic dissipation or adiabatic compression, but this is harder to recognize observationally. The energy that appears in the corona ultimately increases the gas pressure there,

which in turn – somewhat counterintuitively – enables chromospheric material to flow up into the corona. The radiation signatures at these different stages spread across the electromagnetic spectrum, as sketched out in Figure 2.1; they are integrated together into the bolometric flare observation shown in Figure 2.3.

The partition of the energy release must also include bulk terms (kinetic energy, gravitational potential energy, and enthalpy). We can readily estimate the kinetic energy of the CME ejecta (e.g., Vourlidas *et al.*, 2000), but the magnetic energy – the dominant term, since electrodynamic forces drive the whole process – is much more difficult. Indeed, a plausible extension of the Aly-Sturrock theorem (Aly, 1991; Sturrock, 1991) suggests that the creation of a CME actually absorbs magnetic energy rather than releasing it, since the open fields it creates are maximally non-potential in nature. So, even the sign of this component of CME energy remains ambiguous. In any case, by order of magnitude, a major flare/CME event may have comparable radiant and bulk kinetic "emissions" (e.g., Emslie *et al.*, 2005; see also Figure 2.6).

2.4.3 Nanoflares

The nature of coronal heating may involve flare-like processes, even outside the times of actual flares or microflares. Parker (1988) introduced the term "nanoflare," implying that just this kind of nonthermal process might be involved in ordinary coronal heating. Here the "nano" implies an event energy on the order of 10^{-9} of that of a major flare, and the suggestion was that a swarm of such tiny events might not be recognizable from a continuous heating process. In general, the possibility that individual elements of a structure are unresolved by a given observation strongly affects its interpretation (Sturrock et al., 1990; Cargill & Klimchuk, 2005).

Hudson (1991) noted that such an occurrence pattern of tiny events would necessarily differ from the "hard" powerlaw seen for true flares (see Section 2.2.5). A single nanoflare could not be detected directly, but the nanoflaring process could be detected statistically from the fluctuation spectrum. In practice most workers ignore this distinction and just view nanoflares as still smaller microflares that can still have individually recognizable signatures.

The concept of nanoflare heating lies close to the interpretation of a flare as an assembly of semi-independent filamentary substructures. This might be expected from the anisotropy of plasma transport properties in the presence of a magnetic field. The arcade structure of many flares indeed shows their inherently filamentary structure, albeit on observable scales. Aschwanden et al. (2001), for example, decomposed a major arcade structure into about 100 individually recognizable strands. This has made "multithread modeling" of

flare structures possible (Hori et al. 1998; Warren 2006), with substantial implications for the physics.

2.5 Flare analogs

In this section we discuss the possible analogies between the forms of solar activity and non-solar phenomena. These often seem striking enough to beg for a common model, but even without success in developing such a model (it would be fair to say that no predictive models for flares now exist) we can certainly use paradigms from one domain as frameworks for understanding another. The two major areas of overlap are the terrestrial aurora and stellar flares, but there are other possible patterns as well.

2.5.1 Other patterns of flare activity

As we have seen, there is a rather well-defined basic observational template for solar flares, both eruptive and confined. The key features include intense non-thermal radiations in an impulsive phase that leads to a gradual phase via the formation of a coronal reservoir (the Neupert Effect). The hard X-ray emission characteristically follows the soft-hard-soft pattern of spectral variation in the impulsive phase. The gradual phase has high temperatures characteristically 1-2 orders of magnitude higher than those of the quiet corona. There is a weak correlation between temperature and emission measure $\int n_e^2 dV$. The chromospheric signatures (e.g., Hα) are dominated by the formation of ribbon structures that tend to spread apart in the gradual phase, reflecting the arcade structure of the flare loops. These properties, and possibly a few others, describe the solar flare paradigm. The stellar flare shown in Figure 2.12 has a clear Neupert-effect time profile. This does not mean very much in terms of the physical distinctions between this event and a solar flare, unfortunately, except to confirm that there a coronal energy reservoir can also form in the vicinity of this star (II Pegasi) as well.

Other patterns of solar activity exist, and these may be more relevant to some non-solar conditions than the standard paradigm. These would include the following (Hudson & Micela, 2006):

Extended events: In major flares, especially those associated with solar energetic particles, an extended later non-thermal phase sometimes develops on time scales of tens of minutes following the impulsive phase. These events have a close relationship with the meter-wave type IV emission, which reveal the presence of relativistic electrons via synchrotron emission (Boischot

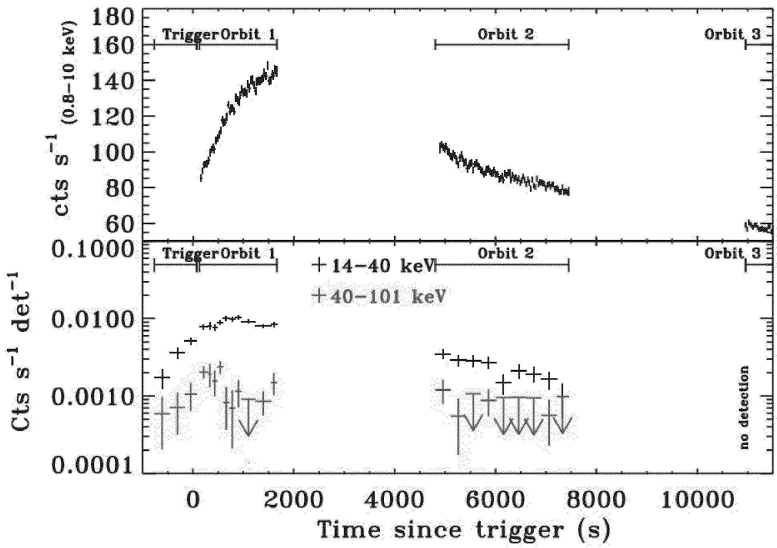

Fig. 2.12. Powerful stellar flare observed 2005 December 16 on the active binary system II Pegasi (Osten et al., 2007). The upper curve shows 0.8-10 keV counting rate from the XRT instrument on board SWIFT (Burrows et al., 2005), and the lower curves show two hard X-ray channels (14-40 keV and 40-101 keV) from the BAT instrument. One can see the clear progression of a Neupert-effect analogy, with the highest-energy channel (lighter shading) showing an impulsive-phase excess in the first ksec of the observation.

& Denisse; see Wild et al. 1963). In the hard X-ray band we see a *soft-hard-harder* spectral evolution (Frost and Dennis, 1971; Hudson, 1978; Cliver *et al.*, 1986) rather than the clear soft-hard-soft evolution of the impulsive phase. Kiplinger (1995) found that this hard X-ray spectral pattern tends to accompany solar proton events. The coronal structures associated with such events are now known to have bright footpoints (Qiu *et al.*, 2004; Krucker *et al.*, 2008), which means that they share some of their physics with the ordinary flare paradigm. But their long duration, great scale, and very high electron energies all suggest a fundamental difference in origin.

Masuda events: The original Masuda event of 1992 January 13 (Masuda *et al.*, 1994) excited enormous interest. Long thought to be prototypical, it now seems to have been rather unusual, with at most a handful of other examples having been observed, either by *Yohkoh* or by RHESSI (Krucker *et al.*, 2008). In this event, *Yohkoh*/HXT observed hard X-ray emission, up to its highest-energy band at 53-93 keV, from a source well above the loops emitting soft X-rays. The Masuda source was therefore termed an "above-the-loop-top" source, distinct from the usual thermal loop-top sources. Because

bremsstrahlung is inefficient, this required a balancing act to explain – could the nonthermal electrons find a high enough density to produce the observed emission, while at the same time remaining remaining trapped? How could the coronal energy release not drive the expected evaporation? The physics remains unclear because of these discrepancies.

Non-thermal ejecta: The meter-wave radio observations provide several examples of distinctly different high-energy processes operating in the solar corona. These include the types I-V bursts (Wild *et al.*, 1963) and now probably some of their counterparts in hard X-rays (Hudson *et al.*, 2001; Krucker *et al.*, 2008). These have great interest at the present time because of their association with CMEs and therefore with disturbances in the Earth's environment.

Coronal thick-target events: In the ordinary flare paradigm, the collisional thick-target model places the target (the hard X-ray source) in the chromosphere. Recently events have been found for which the best interpretation is that the fast electrons actually do not propagate as far as the chromosphere, but instead brake collisionally in the corona (Veronig and Brown, 2004). This development was unexpected because of the general success of the standard model (see Chapter 3), and it suggests that the powerful electron acceleration of the impulsive phase can take place in a relatively high-density medium ($n_e > 10^{10}$ cm^{-3}), in order to provide enough coronal column density to bring a $\sim$50 keV electron to rest.

Shock waves: This mechanism is of particular interest in astrophysics, where there is hardly a domain on any scale in which shock physics is not applicable. In the case of the solar flare, we are particularly interested in large-scale waves that accompany the basic restructuring of the field needed to release energy. Note that in 2D Petschek reconnection it is precisely the large-scale shock waves that convert the magnetic energy; the reconnection point itself is of little consequence for energy release. We do not know yet whether or not this logic carries over to non-steady 3D magnetic reconnection. The large-scale shock waves in solar flares can readily be detected via their radio emission. We understand the physics of a type II burst well enough to identify it as the emission signature as the product of Langmuir turbulence scattering energy into electromagnetic radiation near the local plasma frequency (Wild *et al.*, 1963) or its harmonic. The shock can occur either near the surface of the Sun, where it may be a blast wave propagating through the ambient, undisturbed corona, or it may be an interplanetary wave driven by the CME. Recently Mewaldt et al. (2007) have obtained the results shown in Figure 2.13 (left).

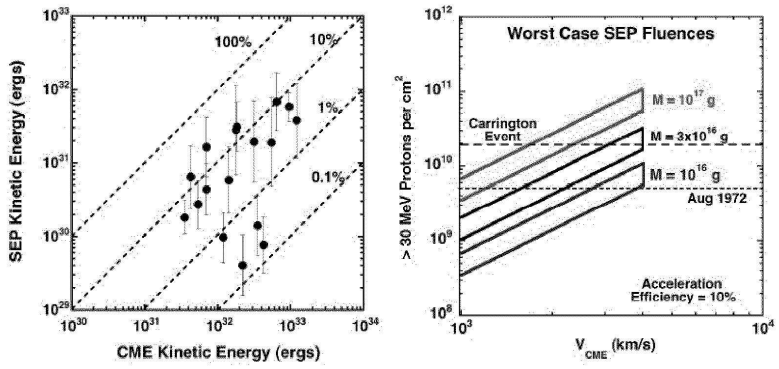

Fig. 2.13. *Left:* Energy converted by interplanetary (CME-driven) shock waves into solar energetic particles (SEPs). The efficiency of conversion can exceed 10%. *Right:* Comparison of particle fluences for model CME masses and speeds, relating the Carrington event to better-observed recent examples (Mewaldt et al., 2007).

Apparently the acceleration of high-energy particles may play a major role in the dissipation of energy at such a collisionless shock. Note that such a mode of energy dissipation is basically a long-range effect: energy is removed from the shock but not converted to heat locally. This means that an ideal MHD simulation will not correctly localize the eventual sink of the shock energy.

Impulse response: White et al. (1992) observed a solar radio burst with quite remarkable properties. With high-resolution VLA observations, the event was located in an active region and had an oblong shape about 5000 km in length and 1500 km in width, thus presumably a compact loop. This, plus oddities in the radio spectrum, place it and a few similar events in a separate category. The small scale presumably means that the event took place in the lowest atmosphere, presumably below the chromosphere-corona interface region. "Impulse response" refers to the emission time profile, which had a nearly unresolved rise time and a brief, exponential, and frequency-independent decay (about 20 s) at 15 GHz.

2.5.2 Aurorae on Earth and elsewhere

The terrestrial aurora is of course a visual phenomenon, but as in a solar flare accelerated particles stimulate much of the radiation. It occurs primarily in an "auroral oval" roughly identified with the boundary between closed magnetospheric magnetic field, and field that opens out into interplanetary space. Jovian aurorae have a similar spatial relationship to the planet's magnetic field, but may in addition have other sources (see the Io-related hot spot in

Figure 13.7, Volume II). Some sort of auroral emission has been detected on the other gas giants (Saturn, Neptune, Uranus) as well as on Venus and Mars; there is at least airglow present even the Jovian moons Europa, Ganymede, and Io Hall *et al.*, 1998. The Jovian auroral X-rays were long sought for, following the terrestrial analogy, and finally found by Metzger et al. (1983).

The terrestrial aurora, especially its "substorm" development, has several points of similarity to the phenomena of solar flares. This has long been noted to be of interest (e.g., Obayashi, 1975; Bratenahl and Baum, 1976; Schindler, 1976; Akasofu, 1979; Akasofu, 2001). Properties that might be related include the acceleration of non-thermal electrons and the identification of N-S conjugate auroral zones as ribbon-like structures. One can note the gradual build-up of stored energy, and its sudden release, as the system evolves past the point of marginal stability. This theoretical idea plus the attractiveness of magnetic reconnection as an energy source for each process have also encouraged this kind of thinking.

Over the decades these possible analogies have retained their fascination, but little has come from this except for a few cartoons. Why is this? Presumably the answer is to be found in the very different physical conditions in the corona and in the geomagnetic tail, even though these parameters scale in such a way that the physical properties are not too dissimilar (e.g., Obayashi, 1975; see Chapter 8 for a full discussion of the physics of planetary magnetospheres). We note that the boundaries of the magnetosphere are the ionosphere and the magnetopause. Along the flanks of the magnetosphere there is a solar-wind flow that creates a large convective electrical potential. This would not be present in the solar corona. The not-so-analogous boundaries of the solar corona are the photosphere/corona transition zone, mainly the chromosphere, and a rather nebulous and ill-understood process that creates the solar wind and decouples it from the coronal plasma. These boundaries have some commonalities (Haerendel, 2006) but some major differences as well. The chromosphere and the ionosphere have different conductivity tensors, and the ionosphere has a non-conducting lower boundary, for example. As for the solar-wind flow around the magnetosphere, there is simply no solar analog. This flow is thought to be the source of the substorm energy, and so the "flare build-up" process seems not to be analogous.

2.5.3 Stellar flares

Many observed light-curve properties of solar and stellar flares resemble one another. There is a tendency for the same fast-rise/slow-decay pattern, a similar relationship between hard and soft X-rays (Osten *et al.*, 2007; Isola *et al.*, 2007) and even a stellar Neupert effect visible in comparisons of white

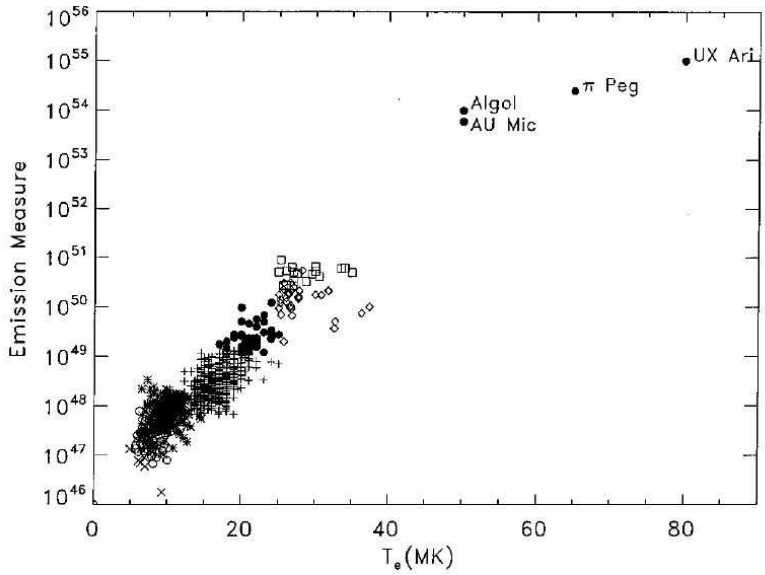

Fig. 2.14. Correlation of temperature and emission measure for solar and stellar flares. The different symbols refer to different data sources, as explained in the original reference (Feldman et al. 2008).

light (Hawley *et al.*, 1995) and microwaves (Guedel *et al.*, 1996) with soft X-ray time profiles. In soft X-rays there is a clear statistical relationship between the emission measure ($\int n_e^2 dV$) and the temperature, as shown in Figure 2.14 (Feldman *et al.*, Aschwanden *et al.*, 1995, 2008). This correlation, first noted by Feldman (1995), while apparently significant, necessarily intercompares very different kinds of observations. The relatively poor correlations seen in individual data sets suggest that systematic biases play an important role, as yet not well understood, independent of the overall correlation. From the point of view of "universal physical processes," it has been argued that this broad correlation results from a universal kind of magnetic reconnection (Shibata and Yokoyama, 1999). This may be an overinterpretation of effects explainable in other ways (Aschwanden *et al.*, 2008), but at a minimum it suggests the importance of the Alfvén speed as a parameter.

The most easily observable stellar flares are found on the traditional dMe flare stars. These stars are cooler and fainter than the Sun (G2V), making it easier to detect brightenings. Indeed the powerful Carrington flare of 1859 would not readily have been detectable if it occurred on a distant G-type star. A stellar flare of comparable magnitude can be readily detected against the background of a much fainter M star photosphere, but that does not explain the observations of much more energetic events seen on other stars (e.g., Schae-

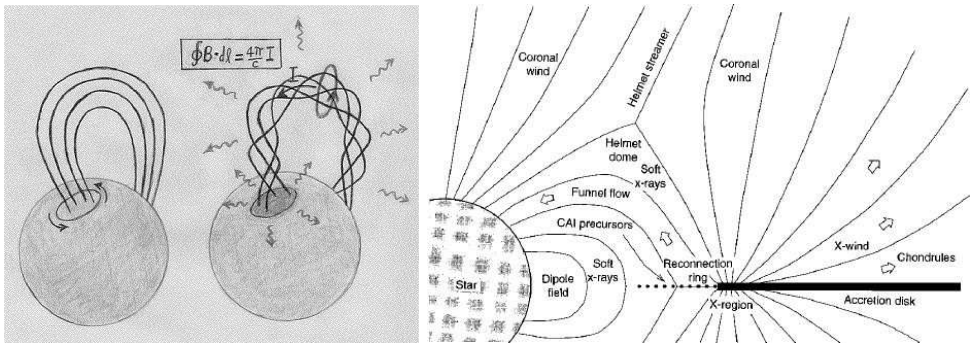

Fig. 2.15. *Left:* Cartoon showing energy storage in the "corona" of a magnetar, a neutron star magnetized to $\sim 10^{15}$ G and capable of giant flares (Duncan, 2005; Duncan et al., 2005). *Right* Cartoon showing "X-wind" model of magnetic fields involved in the accretion of matter onto a young star (Shu et al., 1997).

fer et al., 2000). This suggests that there may be something quantitatively different about the stellar flares or their causes.

Figure 2.12 shows a flare observed from the active binary system II Pegasi (presumably the K subgiant component; Osten *et al.*, 2007). In general the binary nature of a stellar system plays a role in its flare productivity, since even many more prosaic dMe flare stars are also binary members. This would then be another distinction from the solar case.

2.5.4 Gamma-ray bursts, magnetar giant flares, and other exotic analogs

Beyond flare stars, which may seem like a safe enough step away from solar experience, there are many other stellar phenomena in which electrodynamics is invoked to explain the observations. Figure 2.15 shows sketches of two examples, which we discuss briefly here. The left panel shows twisted field lines hypothesized to develop in the atmosphere of a "magnetar," a neutron star thought to have interior magnetic-field strengths as large as 10^{15} G (Thompson and Duncan, 1995). The rough idea is that magnetic energy can build up in these twists, maintained by the rigidity of the neutron-star crust, until a giant flare releases it. The right panel is a representation of the "X wind" model of Shu et al. (1997), which generalizes the solar ideas by involving the accretion disk of a young star (T Tauri) in the stressing of the field and its release as a flare. The high activity of young stars presumably results from rapid rotation and the presence of an accretion disk.

2.6 Magnetic reconnection, observationally

2.6.1 Connectivity

Although magnetic reconnection is only one possible way to extract energy from a magnetic field, this idea dominates most research in flare theory. Most observers therefore try to understand their observations in this way. I take this opportunity to discuss how to detect the process of reconnection, appreciating that in a laboratory, or in an *in situ* observation in space, one can actually get down to the relevant scales at which particles "demagnetize" and reconnection can happen. This is unlikely ever to be the case for astronomical observations, unfortunately; the proton inertial length c/ω_{pi} is tiny, approximately 10^3 cm at the top of the VAL-C (Vernazza *et al.*, 1981) chromosphere (Hudson, 2007a).

The best evidence for the occurrence of reconnection, therefore, must come from tracking connectivity, via the identification of magnetic domains (see the full discussion Longcope, 2009). A flare driven by reconnection would involve the transfer of flux between two domains of different connectivity, in such a manner as to release some fraction of the stored energy. But how to identify the domains? This can really only be done in the context of a coronal magnetic-field model at a level of approximation that permits stresses to remain in the field, and hence separate domains to exist. A field model derivable from a scalar potential will not serve perfectly, but if the coronal field is only weakly non-potential, the separatrices between the domains may be in about the right places.

In a large-scale magnetic reconnection model, one might expect the flare brightenings to appear at the intersections of coronal magnetic separatrix surfaces with the photosphere. The separatrices show the location of sudden changes in the connectivity maps (Titov and Démoulin, 1999). Mandrini *et al.* (1991) had observed Hα brightenings at such locations, and recently Metcalf *et al.* (2003) presented an excellent example of this for the flare shown in Figure 2.9 (right). Figure 2.16 shows the mapping for this event. Such indirect correspondences provide some of the best evidence to date of the large-scale reconnection picture, but note that the observation is still quite remote from the microphysics of reconnection, and that there are necessarily ambiguities in the interpretation.

Many other flare observations have been interpreted in terms of large-scale magnetic reconnection. The "Masuda flare" (Masuda *et al.*, 1994) is often cited as conclusive evidence for such a picture, and a more recent *Yohkoh* observation of apparent reconnection inflow (Yokoyama *et al.*, 2001) also fits the picture. However, each of these events was quite unusual and may have drawn attention not so much because they were in any sense typical, but

Fig. 2.16. Mapping of separatrices to the photosphere (heavy lines) compared with hard X-ray footpoint locations (crosses) for the flare of 2001 August 25 (Metcalf et al. 2003), also the subect of Figure 2.9b. The image dimensions are 120 × 150 arc sec in X and Y, respectively. The main flare ribbons are at the upper part of the figure, but note how faithfully the remote brightenings follow the projected separatrix at the bottom of the figure as well.

simply because they evoked the cartoon. In the *Yohkoh* era, probably the best circumstantial evidence for reconnection dynamics was in the observation of the "supra-arcade downflows" (McKenzie and Hudson, 1999; McKenzie, 2000; Asai *et al.*, 2004b). Recently Hara et al. (2008) have applied the much better observational material of the *Hinode*/EIS instrument (Culhane *et al.*, 2007) to a well-observed gradual flare. In principle, such observations would show the reconnection flow fields and thus be a step closer to confirming the reality of the picture. Such an observation appears to have been too difficult even for this instrument, at least for this flare, and no unambiguous results could be obtained.

In general the observations most strongly suggestive of the reconnection picture apply mainly to the later phases of a flare. Asai et al. (2004) observed supra-arcade downflows in coincidence with hard X-ray bursts in the flare of 2002 July 23,) but it is not clear yet exactly how to apply the idea of magnetic reconnection to the impulsive phase, or to flares without eruptions.

2.6.2 Current sheets

Magnetic reconnection requires the existence of a current sheet on a scale fine enough for particle demagnetization to occur. Given the small values of the ion inertial length ($c/\omega_p i \ll 1$ km in the corona), the detectability of a current sheet would be indirect by any known remote-sensing technique. Enhanced density or temperature could be clues, for example, or simple image morphology based on theoretical expectation.

For some CMEs there is clear evidence for the re-formation of a coronal helmet streamer following the event (Kahler & Hundhausen, 1992; Hiei et al., 1993). We interpret this to mean that the juxtaposed open fields of opposite polarities do form an active current sheet during a reconnection process. Webb et al. (2003) discuss this CME morphology in detail.

Temperature and density signatures might also be expected in the EUV or soft X-ray ranges, given the dynamics of the reconnecting magnetic field, especially in flares for which the process might be faster and more energetic. These physical parameters translate into an emission measure $n_e n_i L$, where L represents the width of the source in the line of sight. Theory or modeling do not give us good predictions for any of these parameters, but UV observations of several linear features behind CMEs strongly suggest that they are in fact the expected current sheets, or else plasma structures closely related to them (see Ciaravella & Raymond, 2008, and other papers cited therein). One distinguishing feature of most of the handful of events detected in this manner is the presence of the high-temperature FeXVIII ion.

X-ray observations of flares with RHESSI have also provided indirect evidence for the presence of current sheets in the impulsive phase of a flare, where reconnection models would expect them (Sui & Holman, 2003; Sui et al., 2004).

2.6.3 Coronal motions

The plasma in the core of an active region has a low plasma β; for reasonable values of the physical parameters we find $\beta = 2\mathrm{nk}_B\mathrm{T}/(\mathrm{B}^2/8\pi)$ to be of order 10^{-4} or lower. This means that any detectable features – any emission at any wavelength – will serve mainly as a "leaf in the wind" (Sheeley *et al.*, 1999), helping us to determine the geometry of the flows but not having much physical significance. The bright features are not important physical objects, since they are embedded in a much stronger and pervasive magnetic field that determines the forces dictating the flow.

The discovery of the "supra-arcade downflows" (McKenzie and Hudson, 1999) offers one of the main possible links between the observations of plasma

motions in the flare and the idea of large-scale magnetic reconnection. This phenomenon is best appreciated in movie format; although it was discovered with *Yohkoh*/SXT soft X-ray observations, in fact the higher resolution available in the TRACE 195Å data make it more visible. The data show a downward flow toward the surface of the Sun from above the developing arcade. The flow speeds are sub-Alfvénic and show deceleration as they approach the arcade loops (McKenzie, 2000; Sheeley *et al.*, 2004). It would be attractive to interpret these motions as confirmation of the standard reconnection model, but the (apparently) highly sub-Alfvénic speeds provide a major obstacle to this interpretation. Asai et al. (2004b) show that such motions can occur even during the impulsive phase of a flare.

Soft X-ray dimming signatures offer another signature. These were another *Yohkoh* discovery (Hudson *et al.*, 1995b; but see Rust, 1979, for earlier *Skylab* observations and Hansen et al. (1974) for still earlier observations from a ground-based coronagraph). The dimming coincides with the impulsive phase of the flare (Zarro *et al.*, 1999) and hence with the acceleration phase of the associated CME (Zhang *et al.*, 2004). It is thus reasonable to associate the dimming signature with the outward flow of mass required by a CME. Although there are many observations now of expanding loops, seen in many wave bands, the dimming signature is more profound and often can be seen in diffuse or unresolved corona. This signature is important for the reconnection models because it identifies newly opened field that can then reconnect.

Some of the dimming may also be related directly to the inflow expected of large-scale reconnection (Yokoyama *et al.*, 2001). In this case the flow field would be essentially horizontal, rather than radially outward as in the "transient coronal hole" interpretation of dimming as the mass being lost to the CME. Measuring the orientation of the velocity field should therefore be a high priority for future spectroscopic observations (via the Doppler effect) and for future high-resolution imaging observations (via "leaves in the wind"). Other examples of this type have been found, but they are rare and do not provide good evidence for a well-understood reconnection scenario in the impulsive phase.

2.6.4 Ribbon motions

The expanding motions of flare ribbons provided one of the first clues to what we think of as the standard reconnection model of a flare (the sketch of Figure 5.4 in Forbes, 2009, or others in Chapter 3 of this volume). As pointed out by Poletto & Kopp (1986), these motions can be interpreted as an electric field. This is a motional or "convective" electric field given by $\mathbf{E} = \mathbf{v} \times \mathbf{B}$, and it is often taken as a measure of the reconnection rate. Fletcher & Hudson (2001)

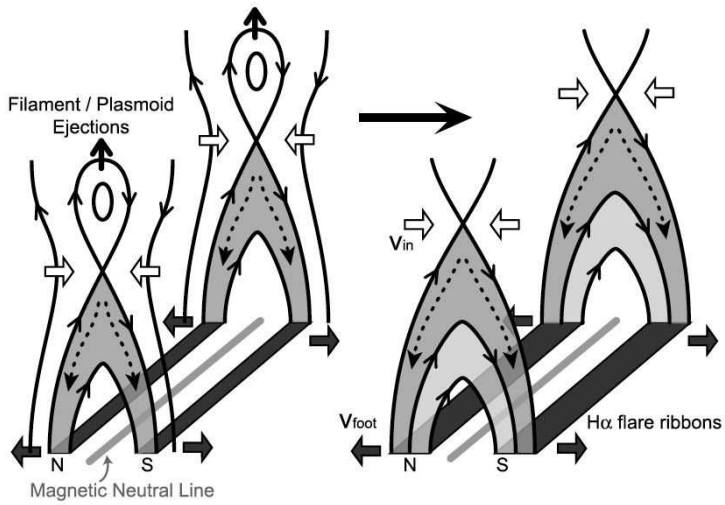

Fig. 2.17. How the ribbon motion sweeps out magnetic field during the reconnection process in the standard model (from Asai et al., 2004a).

point out that the rate the ribbons sweep out the field should correspond in some sense to the rate at which energy is released during reconnection, and that at the same time the field guides the particle or heat flux responsible for the ribbon excitation. Figure 2.17 shows the geometry.

The actual magnitude the convective field may be quite large. We can estimate it (in SI units for convenience) for a reconnection flow speed $|\mathbf{v}| = 0.1\ \mathrm{v}_A$, where v_A is the Alfvén speed, which would plausibly be $\mathrm{v}_A = 10^7$ m/s in the core of an active region. Then for $|\mathbf{B}| = 0.1$ T, $|\mathbf{E}| = 10^6$ V/m. Similarly the Poynting flux can be estimated at 10^5 W/m^2 (e.g., Asai *et al.*, 2004a), approximately the level needed to power a flare with plausible assumptions about the geometry. Asai et al. (2004a) also showed that the local Poynting flux appeared to correlate in time with the temporal variations of impulsive-phase signatures, consistent with expectation from the standard reconnection model.

2.6.5 Particle acceleration

How does one understand particle acceleration in the context of magnetic reconnection, and can the particles be a guide to understanding the reconnection physics? At first glance this may seem implausible, since one frequently appeals to reconnection within an MHD framework, as in Figure 2.17. MHD is a fluid theory and therefore has no particles at all, and so any theory of particle acceleration needs to be grafted on in a non-self-consistent manner as a

"test-particle" theory. This would be satisfactory theoretically if the particles were energetically unimportant, but as we have seen (Section 2.2.2) this is not true in the impulsive phase at least.

It is also tempting to take the convective electric field $\mathbf{E} = \mathbf{v}\times\mathbf{B}$ as a mechanism for particle acceleration, but strictly speaking this is wrong because the convective field has zero $\mathbf{E}_{\|}$ component. Nevertheless one can imagine situations, in the absence of a detailed theory of reconnection, in which the current sheet can in fact accelerate particles. Speiser (1965) showed how this would readily happen via non-adiabatic motions (e.g., Northrop and Teller, 1960) in the "Speiser orbits." A current-sheet mechanism as a source of the 10-100 keV electrons of the impulsive phase immediately has trouble with the "number problem," though, since the inferred intensities of the electron beams in the thick-target model are so high.

Several other ways to link the standard reconnection model with the requirement for particle acceleration have been proposed. It is natural to consider a role for shock waves associated with the reconnection. In Petschek 2D reconnection, in fact, the energy is converted to flows at a pair of standing slow-mode shocks; the flows themselves could terminate at standing fast-mode shocks as well. Tsuneta & Naito (1998) used the latter for acceleration and the former for trapping. Unfortunately there is no clear evidence for fast reconnection outflows and their attendant fast-mode shocks (see Section 2.6.3). This theory may then fail as a result of the 2D reconnection picture not providing a good approximation to the 3D situation.

Recently Fletcher & Hudson (2008) have introduced ideas carried over from the terrestrial aurora and somewhat new to solar physics. These ideas, sketched in Figure 2.18, make use of the Poynting flux of Alfvén waves generated in the restructuring of the coronal magnetic field (Emslie and Sturrock, 1982). The particle acceleration would hypothetically result from the development of structure on small scales, generating the necesssary $|\mathbf{E}_{\|}|$ either via kinetic effects in the wave propagation (e.g., Kletzing, 1994) or via the development of turbulence (e.g., Larosa *et al.*, 1994; Petrosian and Liu, 2004). In either case, the actual particle acceleration could take place near the chromosphere and thus have a better chance to avoid the number problem.

2.7 Conclusions

This Chapter has reviewed the status of our observational material on solar flares, including other forms of solar activity and some of their analogs in other environments. Observations of flares now span parts of three centuries, and many things have been learned. Nevertheless major questions remain unanswered, and so the observations must be improved. What do we not under-

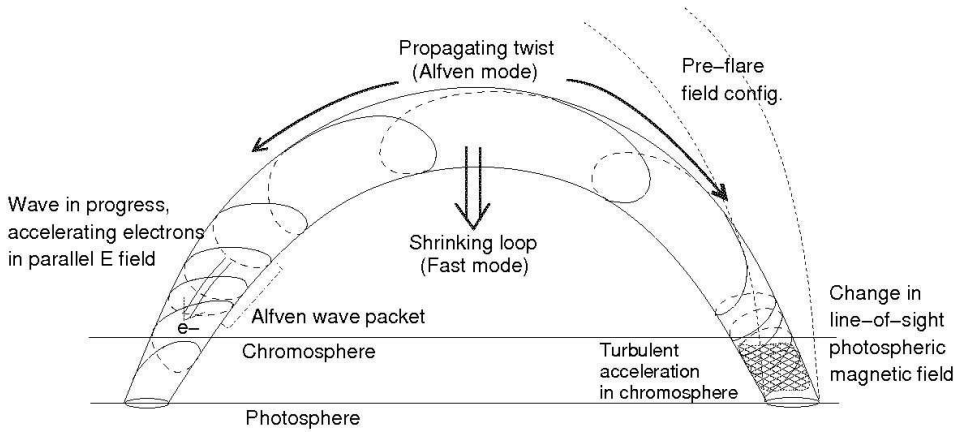

Fig. 2.18. Model put forth by Fletcher & Hudson (2008), showing the extraction of stored coronal magnetic energy via the Poynting flux of waves excited by the restructuring that produces the flare. Particle acceleration in this picture, as in other pictures, remains problematic.

stand, and how should we proceed to learn more? I will start this conclusion with some general remarks and then get specific about the observations.

Flares are are a clear example of a "stick and slip" process, whereby energy builds up slowly and then converts suddenly into other forms. In this case the storage is in the inductive magnetic field of currents driven into the solar atmosphere by convective motions in the solar interior. These currents can find quasi-stable equilibria that evolve until a loss of equilibrium takes place. The energy release in the resulting development of the system is nonlinear and involves a range of scales in the plasma that cannot be described quantitatively at the present time. We thus do not have a predictive theory of the restructuring that releases this stored coronal energy and results in a flare. The paramount problem of flare physics therefore is to understand the transformation of energy in this interesting physical system.

The physical essence of flare physics, regarded most generally, would be in the behavior of the interface between a stellar interior and its atmosphere. The Sun shows us that this interface reacts in quite striking ways to what should be an orderly flow of stellar energy away from its interior sources. Electrodynamic effects dominate the interaction between this flow and the exterior space. For the Sun, the flare is the most common of these effects in terms of coronal signatures. For the most energetic flares the simultaneous occurrence of a CME and its concomitant particle acceleration leads to physically (and perhaps biologically!) important interactions with planetary environments. In a separate article (Hudson, 2007a), I have recently reviewed the state of

our knowledge of the flare chromosphere. We do not know enough, in spite of a long history of observation! Following the premise of Harwit (1981), we should note that there is a vast unobserved parameter space in the UV and EUV wavelength ranges covering these regions of the solar atmosphere. Harwit argued that cosmic discovery follows almost directly from the opening-up of new parameter domains. The most striking omission in the case of solar flares might be the almost complete lack of hydrogen Lyα observations with sufficiently high spectral, spatial, and temporal coverage. Note that this is the most basic spectral line of the most abundant element on the nearest star!

Other important omissions include sensitive observations, at high resolution, of X and γ-rays. The most direct insight into flare energy release necessarily must follow from observation of the accelerated particles. In this context radio techniques also have great sensitivity and a parameter space that has not been exploited. Specifically in the microwave band, we have never had sensitive broad-band spectral coverage. Almost all of the observations to date have been at widely spaced fixed frequencies that provide only limited information about the physical properties of the sources, including the all-important coronal magnetic field (e.g., Brosius and White, 2006).

13
Energetic particles and technology

by Alan Tribble

Bibliography

Abbett, W. P.: 2007, ApJ 665, 1469

Akabane, K.: 1956, Publ. Ast. Soc. Japan 8, 173

Akasofu, S.-I.: 1979, Solar Phys. 64, 333

Akasofu, S.-I.: 2001, Space Science Reviews 95, 613

Aly, J. J.: 1991, Ap. J. Lett. 375, L61

Asai, A., Yokoyama, T., Shimojo, M., Masuda, S., Kurokawa, H., & Shibata, K.: 2004a, Ap. J. 611, 557

Asai, A., Yokoyama, T., Shimojo, M., & Shibata, K.: 2004b, Ap. J. Lett. 605, L77

Aschwanden, M. J. & Alexander, D.: 2001, Solar Phys. 204, 91

Aschwanden, M. J., Stern, R. A., & Güdel, M.: 2008, Ap. J. 672, 659

Athay, R. G. & Moreton, G. E.: 1961, Ap. J. 133, 935

Aurass, H., Klein, K.-L., & Martens, P. C. H.: 1994, Solar Phys. 155, 203

Bastian, T. S., Benz, A. O., & Gary, D. E.: 1998, Astron. Astrophys. 36, 131

Benz, A. (Ed.): 2002, *Plasma Astrophysics, second edition*, Vol. 279 of *Astrophysics and Space Science Library*

Biesecker, D. A., Myers, D. C., Thompson, B. J., Hammer, D. M., & Vourlidas, A.: 2002, Ap. J. 569, 1009

Billings, D. E.: 1966, *A guide to the solar corona*, New York: Academic Press, —c1966

Bratenahl, A. & Baum, P. J.: 1976, Solar Phys. 47, 345

Brosius, J. W. & White, S. M.: 2006, Ap. J. Lett. 641, L69

Brown, J. C.: 1971, Solar Phys. 18, 489

Brown, J. C. & Mallik, P. C. V.: 2008, Astron. Astrophys. 481, 507

Burkepile, J. T., Hundhausen, A. J., Stanger, A. L., St. Cyr, O. C., & Seiden, J. A.: 2004, Journal of Geophysical Research (Space Physics) 109(A18), 3103

Burrows, D. N., Hill, J. E., Nousek, J. A., Kennea, J. A., Wells, A., Osborne, J. P., Abbey, A. F., Beardmore, A., Mukerjee, K., Short, A. D. T., Chincarini, G., Campana, S., Citterio, O., Moretti, A., Pagani, C., Tagliaferri, G., Giommi, P., Capalbi, M., Tamburelli, F., Angelini, L., Cusumano, G., Bräuninger, H. W., Burkert, W., & Hartner, G. D.: 2005, Space Science Reviews 120, 165

Cargill, P. J. & Klimchuk, J. A.: 2004, Ap. J. 605, 911

Carrington, R. C.: 1859, Mon. Not. r. Ast. Soc. 20, 13

Chapman, S. & Bartels, J.: 1940, *Geomagnetism*, Oxford: University Press, 1940

Chifor, C., Tripathi, D., Mason, H. E., & Dennis, B. R.: 2007, Astron. Astrophys. 472, 967

Christe, S., Hannah, I. G., Krucker, S., McTiernan, J., & Lin, R. P.: 2008, Ap. J. 677, 1385

Ciaravella, A. & Raymond, J. C.: 2008, Ap. J. 686, 1372

Cliver, E. W.: 1995, Solar Phys. 157, 285

Cliver, E. W., Dennis, B. R., Kiplinger, A. L., Kane, S. R., Neidig, D. F., Sheeley, Jr., N. R., & Koomen, M. J.: 1986, Ap. J. 305, 920

Crockett, W. R., Purcell, J. D., Schumacher, R. J., Tousey, R., & Patterson, N. P.: 1977, Applied Optics 16, 893

Crosby, N. B., Aschwanden, M. J., & Dennis, B. R.: 1993, Solar Phys. 143, 275

Culhane, J. L., Harra, L. K., James, A. M., Al-Janabi, K., Bradley, L. J., Chaudry, R. A., Rees, K., Tandy, J. A., Thomas, P., Whillock, M. C. R., Winter, B., Doschek, G. A., Korendyke, C. M., Brown, C. M., Myers, S., Mariska, J., Seely, J., Lang, J., Kent, B. J., Shaughnessy, B. M., Young, P. R., Simnett, G. M., Castelli, C. M., Mahmoud, S., Mapson-Menard, H., Probyn, B. J., Thomas, R. J., Davila, J., Dere, K., Windt, D., Shea, J., Hagood, R., Moye, R., Hara, H., Watanabe, T., Matsuzaki, K., Kosugi, T., Hansteen, V., & Wikstol, Ø.: 2007, Solar Phys. 243, 19

Dennis, B. R. & Zarro, D. M.: 1993, Solar Phys. 146, 177

Drake, J. F.: 1971, Solar Phys. 16, 152

Duncan, R. C.: 2005, Sky & Telescope 109(1), 010000

Emslie, A. G., Dennis, B. R., Holman, G. D., & Hudson, H. S.: 2005, Journal of Geophysical Research (Space Physics) 110(A9), 11103

Emslie, A. G. & Sturrock, P. A.: 1982, Solar Phys. 80, 99

Engvold, O.: 1989, in E. R. Priest (Ed.), *Dynamics and Structure of Quiescent Solar Prominences*, Vol. 150 of *Astrophysics and Space Science Library*, p. 47

Fárník, F., Hudson, H., & Watanabe, T.: 1996, Solar Phys. 165, 169

Fárník, F., Hudson, H. S., Karlický, M., & Kosugi, T.: 2003, Astron. Astrophys. 399, 1159

Fárník, F. & Savy, S. K.: 1998, Solar Phys. 183, 339

Feldman, U., Laming, J. M., & Doschek, G. A.: 1995, Ap. J. Lett. 451, L79+

Fletcher, L., Hannah, I. G., Hudson, H. S., & Metcalf, T. R.: 2007, Ap. J. 656, 1187

Fletcher, L. & Hudson, H.: 2001, Solar Phys. 204, 69

Fletcher, L. & Hudson, H. S.: 2008, Ap. J. 675, 1645

Forbes, T. G.: 2009, in C. J. Schrijver and G. L. Siscoe (Eds.), *Heliophysics I: Plasma physics of the local cosmos*, Cambridge University Press

Forbes, T. G. & Acton, L. W.: 1996, Ap. J. 459, 330

Frost, K. J. & Dennis, B. R.: 1971, Ap. J. 165, 655

Gaizauskas, V.: 1989, Solar Phys. 121, 135

Gary, G. A.: 1989, Ap. J. Suppl. 69, 323

Gibson, S. E. & Fan, Y.: 2006, Journal of Geophysical Research (Space Physics) 111(A10), 12103

Guedel, M., Benz, A. O., Schmitt, J. H. M. M., & Skinner, S. L.: 1996, Ap. J. 471, 1002

Haerendel, G.: 2006, Space Science Reviews 124, 317

Hale, G. E.: 1930, Ap. J. 71, 73

Hall, D. T., Feldman, P. D., McGrath, M. A., & Strobel, D. F.: 1998, Ap. J. 499, 475

Hannah, I. G., Christe, S., Krucker, S., Hurford, G. J., Hudson, H. S., & Lin, R. P.: 2008, Ap. J. 677, 704

Hansen, R. T., Garcia, C. J., Hansen, S. F., & Yasukawa, E.: 1974, Publ. Ast. Soc. Pacific 86, 500

Hansteen, V. H.: 2009, in C. J. Schrijver and G. L. Siscoe (Eds.), *Heliophysics I: Plasma physics of the local cosmos*, Cambridge University Press

Hara, H., Watanabe, T., Matsuzaki, K., Harra, L. K., Culhane, J. L., Cargill, P., Mariska, J. T., & Doschek, G. A.: 2008, Publ. Ast. Soc. Japan 60, 275

Harvey, K. L., Sheeley, N. R., & Harvey, J. W.: 1986, Solar-Terrestrial Predictions, Volume 2nd, Meudon, France, 18-22 June, 1984. P.A. Simon et al, p. 198-203 2, 198

Harwit, M.: 1981, *Cosmic discovery. The search, scope, and heritage of astronomy*, Brighton: Harvester Press, 1981

Hawley, S. L., Fisher, G. H., Simon, T., Cully, S. L., Deustua, S. E., Jablonski, M., Johns-Krull, C. M., Pettersen, B. R., Smith, V., Spiesman, W. J., & Valenti, J.: 1995, Ap. J. 453, 464

Hey, J. S., Parsons, S. J., & Phillips, J. W.: 1948, Mon. Not. r. Ast. Soc. 108, 354

Heyvaerts, J., Priest, E. R., & Rust, D. M.: 1977, Ap. J. 216, 123

Hiei, E., Hundhausen, A. J., & Sime, D. G.: 1993, Geophys. Res. Lett.20, 2785

Hori, K., Yokoyama, T., Kosugi, T., & Shibata, K.: 1998, Ap. J. 500, 492

Hudson, H., Haisch, B., & Strong, K. T.: 1995a, Journ. Geophys. Res. 100, 3473

Hudson, H. S.: 1972, Solar Phys. 24, 414

Hudson, H. S.: 1978, Ap. J. 224, 235

Hudson, H. S.: 1987, Solar Phys. 113, 1

Hudson, H. S.: 1988, Astron. Astrophys. 26, 473

Hudson, H. S.: 1991, Solar Phys. 133, 357

Hudson, H. S.: 2000, Ap. J. Lett. 531, L75

Hudson, H. S.: 2007a, in P. Heinzel, I. Dorotovič, and R. J. Rutten (Eds.), *The Physics of Chromospheric Plasmas*, Vol. 368 of *Astronomical Society of the Pacific Conference Series*, p. 365

Hudson, H. S.: 2007b, Ap. J. Lett. 663, L45

Hudson, H. S., Acton, L. W., Alexander, D., Freeland, S. L., Lemen, J. R., & Harvey, K. L.: 1995b, in *Solar Wind Eigt*, p. 58

Hudson, H. S. & Cliver, E. W.: 2001, Journ. Geophys. Res. 106, 25199

Hudson, H. S., Hannah, I. G., DeLuca, E. E., & Weber, M.: 2008, AIP

Hudson, H. S., Khan, J. I., Lemen, J. R., Nitta, N. V., & Uchida, Y.: 2003, Solar Phys. 212, 121

Hudson, H. S., Kosugi, T., Nitta, N. V., & Shimojo, M.: 2001, Ap. J. Lett. 561, L211

Hudson, H. S. & Micela, G.: 2006, in *14th Cambridge Workshop on Cool Stars, Stellar Systems and the Sun* (poster)

Hudson, H. S. & Ohki, K.: 1972, Solar Phys. 23, 155

Hudson, H. S., Wolfson, C. J., & Metcalf, T. R.: 2006, Solar Phys. 234, 79

Hundhausen, A.: 1999, in K. T. Strong, J. L. R. Saba, B. M. Haisch, and J. T. Schmelz (Eds.), *The many faces of the sun: a summary of the results from NASA's Solar Maximum Mission.*, p. 143

Hundhausen, A. J., Burkepile, J. T., & St. Cyr, O. C.: 1994, Journ. Geophys. Res. 99, 6543

Hurley, K., Boggs, S. E., Smith, D. M., Duncan, R. C., Lin, R., Zoglauer, A., Krucker, S., Hurford, G., Hudson, H., Wigger, C., Hajdas, W., Thompson, C., Mitrofanov, I., Sanin, A., Boynton, W., Fellows, C., von Kienlin, A., Lichti, G., Rau, A., & Cline, T.: 2005, Nature 434, 1098

Isola, C., Favata, F., Micela, G., & Hudson, H. S.: 2007, Astron. Astrophys. 472, 261

Kahler, S. W.: 1982, Journ. Geophys. Res. 87, 3439

Kane, S. R. & Anderson, K. A.: 1970, Ap. J. 162, 1003

Kane, S. R. & Donnelly, R. F.: 1971, Ap. J. 164, 151

Khan, J. I. & Aurass, H.: 2002, Astron. Astrophys. 383, 1018
Kiplinger, A. L.: 1995, Ap. J. 453, 973
Kletzing, C. A.: 1994, Journ. Geophys. Res. 99, 11095
Kosovichev, A. G. & Zharkova, V. V.: 1998, Nature 393, 317
Kosovichev, A. G. & Zharkova, V. V.: 1999, Solar Phys. 190, 459
Krucker, S., Battaglia, M., Cargill, P. J., Fletcher, L., Hudson, H. S., MacKinnon, A. L., Masuda, S., Sui, L., Tomczak, M., Veronig, A. M., Vlahos, L., & White, S. M.: 2008, Astron. Astrophys. Rev.
Krucker, S., Kontar, E. P., Christe, S., & Lin, R. P.: 2007, Ap. J. Lett. 663, L109
Kundu, M. R.: 1965, *Solar radio astronomy*, New York: Interscience Publication, 1965
Kundu, M. R., Raulin, J. P., Nitta, N., Hudson, H. S., Shimojo, M., Shibata, K., & Raoult, A.: 1995, Ap. J. Lett. 447, L135+
Larosa, T. N., Moore, R. L., & Shore, S. N.: 1994, Ap. J. 425, 856
Lin, H., Penn, M. J., & Tomczyk, S.: 2000, Ap. J. Lett. 541, L83
Lin, R. P.: 1974, Space Science Reviews 16, 189
Lin, R. P. & Hudson, H. S.: 1971, Solar Phys. 17, 412
Lin, R. P. & Hudson, H. S.: 1976, Solar Phys. 50, 153
Liu, C., Deng, N., Liu, Y., Falconer, D., Goode, P. R., Denker, C., & Wang, H.: 2005, Ap. J. 622, 722
Longcope, D.: 2009, in C. J. Schrijver and G. L. Siscoe (Eds.), *Heliophysics I: Plasma physics of the local cosmos*, Cambridge University Press
Machado, M. E. & Linsky, J. L.: 1975, Solar Phys. 42, 395
Mandrini, C. H., Demoulin, P., Henoux, J. C., & Machado, M. E.: 1991, Astron. Astrophys. 250, 541
Martin, S., Panasenco, O., Engvold, O., & Lin, Y.: 2008, Ann. Geophys. ??
Masuda, S., Kosugi, T., Hara, H., Tsuneta, S., & Ogawara, Y.: 1994, Nature 371, 495
McKenzie, D. E.: 2000, Solar Phys. 195, 381
McKenzie, D. E. & Hudson, H. S.: 1999, Ap. J. Lett. 519, L93
Melrose, D. B.: 1992, Ap. J. 387, 403
Metcalf, T. R., Alexander, D., Hudson, H. S., & Longcope, D. W.: 2003, Ap. J. 595, 483
Metzger, A. E., Gilman, D. A., Luthey, J. L., Hurley, K. C., Schnopper, H. W., Seward, F. D., & Sullivan, J. D.: 1983, Journ. Geophys. Res. 88, 7731
Mewaldt, R. A., Cohen, C. M. S., Haggerty, D. K., Mason, G. M., Looper, M. L., von Rosenvinge, T. T., & Wiedenbeck, M. E.: 2007, in *Turbulence and Nonlinear Processes in Astrophysical Plasmas*, Vol. 932 of *American Institute of Physics Conference Series*, p. 277
Moore, R. L. & Labonte, B. J.: 1980, in K. V. Sheridan and G. A. Dulk (Eds.), *Solar and Interplanetary Dynamics*, Vol. 91 of *IAU Symposium*, p. 207
Moses, D., Clette, F., Delaboudiniere, J.-P., Artzner, G. E., Bougnet, M., Brunaud, J., Carabetian, C., Gabriel, A. H., Hochedez, J. F., Millier, F., Song, X. Y., Au, B., Dere, K. P., Howard, R. A., Kreplin, R., Michels, D. J., Defise, J. M., Jamar, C., Rochus, P., Chauvineau, J. P., Marioge, J. P., Catura, R. C., Lemen, J. R., Shing, L., Stern, R. A., Gurman, J. B., Neupert, W. M., Newmark, J., Thompson, B., Maucherat, A., Portier-Fozzani, F., Berghmans, D., Cugnon, P., van Dessel, E. L., & Gabryl, J. R.: 1997, Solar Phys. 175, 571
Nakajima, H. & Yokoyama, T.: 2002, Ap. J. Lett. 570, L41
Neupert, W. M.: 1968, ApJ 153, L59
Nitta, N. V. & Hudson, H. S.: 2001, Geophys. Res. Lett.28, 3801

Northrop, T. G. & Teller, E.: 1960, Physical Review 117, 215
Obayashi, T.: 1975, Solar Phys. 40, 217
Osten, R. A., Drake, S., Tueller, J., Cummings, J., Perri, M., Moretti, A., & Covino, S.: 2007, Ap. J. 654, 1052
Pallavicini, R., Serio, S., & Vaiana, G. S.: 1977, Ap. J. 216, 108
Palmer, I. D. & Smerd, S. F.: 1972, Solar Phys. 26, 460
Parker, E. N.: 1988, Ap. J. 330, 474
Petrosian, V. & Liu, S.: 2004, Ap. J. 610, 550
Poletto, G. & Kopp, R. A.: 1986, in *The Lower Atmosphere of Solar Flares; Proceedings of the Solar Maximum Mission Symposium*, p. 453
Qiu, J., Lee, J., & Gary, D. E.: 2004, Ap. J. 603, 335
Ramaty, R., Mandzhavidze, N., Kozlovsky, B., & Murphy, R. J.: 1995, Ap. J. Lett. 455, L193+
Reames, D. V.: 1999, Space Science Reviews 90, 413
Rust, D. M.: 1979, in *Physics of Solar Prominences*, p. 252
Rust, D. M., Sakurai, T., Gaizauskas, V., Hofmann, A., Martin, S. F., Priest, E. R., & Wang, J.-X.: 1994, Solar Phys. 153, 1
Schaefer, B. E., King, J. R., & Deliyannis, C. P.: 2000, Ap. J. 529, 1026
Schindler, K.: 1976, Solar Phys. 47, 91
Schrijver, C. J.: 2007, Ap. J. Lett. 655, L117
Schrijver, C. J., DeRosa, M. L., Metcalf, T., Barnes, G., Lites, B., Tarbell, T., McTiernan, J., Valori, G., Wiegelmann, T., Wheatland, M. S., Amari, T., Aulanier, G., Démoulin, P., Fuhrmann, M., Kusano, K., Régnier, S., & Thalmann, J. K.: 2008, Ap. J. 675, 1637
Share, G. H., Murphy, R. J., Smith, D. M., Schwartz, R. A., & Lin, R. P.: 2004, Ap. J. Lett. 615, L169
Sheeley, N. R., Walters, J. H., Wang, Y.-M., & Howard, R. A.: 1999, Journ. Geophys. Res. 104, 24739
Sheeley, Jr., N. R., Warren, H. P., & Wang, Y.-M.: 2004, Ap. J. 616, 1224
Shibata, K., Ishido, Y., Acton, L. W., Strong, K. T., Hirayama, T., Uchida, Y., McAllister, A. H., Matsumoto, R., Tsuneta, S., Shimizu, T., Hara, H., Sakurai, T., Ichimoto, K., Nishino, Y., & Ogawara, Y.: 1992, Publ. Ast. Soc. Japan 44, L173
Shibata, K., Nakamura, T., Matsumoto, T., Otsuji, K., Okamoto, T. J., Nishizuka, N., Kawate, T., Watanabe, H., Nagata, S., UeNo, S., Kitai, R., Nozawa, S., Tsuneta, S., Suematsu, Y., Ichimoto, K., Shimizu, T., Katsukawa, Y., Tarbell, T. D., Berger, T. E., Lites, B. W., Shine, R. A., & Title, A. M.: 2007, Science 318, 1591
Shibata, K. & Yokoyama, T.: 1999, Ap. J. Lett. 526, L49
Shimojo, M., Hashimoto, S., Shibata, K., Hirayama, T., Hudson, H. S., & Acton, L. W.: 1996, Publ. Ast. Soc. Japan 48, 123
Shimojo, M., Shibata, K., & Harvey, K. L.: 1998, Solar Phys. 178, 379
Shu, F. H., Shang, H., Glassgold, A. E., & Lee, T.: 1997, Science 277, 1475
Speiser, T. W.: 1965, Journ. Geophys. Res. 70, 4219
Steiner, O.: 2007, ArXiv e-prints 709
Strong, K. T., Harvey, K., Hirayama, T., Nitta, N., Shimizu, T., & Tsuneta, S.: 1992, Publ. Ast. Soc. Japan 44, L161
Sturrock, P. A.: 1991, Ap. J. 380, 655
Sturrock, P. A., Dixon, W. W., Klimchuk, J. A., & Antiochos, S. K.: 1990, Ap. J. Lett. 356, L31
Sudol, J. J. & Harvey, J. W.: 2005, Ap. J. 635, 647

Sui, L. & Holman, G. D.: 2003, Ap. J. Lett. 596, L251
Sui, L., Holman, G. D., & Dennis, B. R.: 2004, Ap. J. 612, 546
Svestka, Z. & Cliver, E. W.: 1992, in Z. Svestka, B. V. Jackson, and M. E. Machado (Eds.), *IAU Colloq. 133: Eruptive Solar Flares*, Vol. 399 of *Lecture Notes in Physics, Berlin Springer Verlag*, p. 1
Thompson, B. J., Gurman, J. B., Neupert, W. M., Newmark, J. S., Delaboudinière, J.-P., St. Cyr, O. C., Stezelberger, S., Dere, K. P., Howard, R. A., & Michels, D. J.: 1999, Ap. J. Lett. 517, L151
Thompson, C. & Duncan, R. C.: 1995, Mon. Not. r. Ast. Soc. 275, 255
Titov, V. S. & Démoulin, P.: 1999, Astron. Astrophys. 351, 707
Tomczyk, S., Card, G. L., Darnell, T., Elmore, D. F., Lull, R., Nelson, P. G., Streander, K. V., Burkepile, J., Casini, R., & Judge, P. G.: 2008, Solar Phys. 247, 411
Tsuneta, S. & Naito, T.: 1998, Ap. J. Lett. 495, L67+
Švestka, Z. F., Fontenla, J. M., Machado, M. E., Martin, S. F., & Neidig, D. F.: 1987, Solar Phys. 108, 237
Uchida, Y.: 1974, Solar Phys. 39, 431
Vernazza, J. E., Avrett, E. H., & Loeser, R.: 1981, Ap. J. Suppl. 45, 635
Veronig, A. M. & Brown, J. C.: 2004, Ap. J. Lett. 603, L117
Veronig, A. M., Karlický, M., Vršnak, B., Temmer, M., Magdalenić, J., Dennis, B. R., Otruba, W., & Pötzi, W.: 2006, Astron. Astrophys. 446, 675
Vorpahl, J. A.: 1973, Solar Phys. 28, 115
Vourlidas, A., Subramanian, P., Dere, K. P., & Howard, R. A.: 2000, Ap. J. 534, 456
Vršnak, B. & Lulić, S.: 2000, Solar Phys. 196, 157
Wang, H., Spirock, T. J., Qiu, J., Ji, H., Yurchyshyn, V., Moon, Y.-J., Denker, C., & Goode, P. R.: 2002, Ap. J. 576, 497
Warren, H. P.: 2006, Ap. J. 637, 522
Webb, D. F.: 1985, Solar Phys. 97, 321
Webb, D. F., Cliver, E. W., Gopalswamy, N., Hudson, H. S., & St. Cyr, O. C.: 1998, Geophys. Res. Lett.25, 2469
Wheatland, M. S., Sturrock, P. A., & Roumeliotis, G.: 2000, Ap. J. 540, 1150
White, S. M.: 2005, in D. E. Innes, A. Lagg, and S. A. Solanki (Eds.), *Chromospheric and Coronal Magnetic Fields*, Vol. 596 of *ESA Special Publication*
White, S. M., Kundu, M. R., Bastian, T. S., Gary, D. E., Hurford, G. J., Kucera, T., & Bieging, J. H.: 1992, Ap. J. 384, 656
Wild, J. P., Smerd, S. F., & Weiss, A. A.: 1963, Astron. Astrophys. 1, 291
Woods, T. N., Kopp, G., & Chamberlin, P. C.: 2006, Journal of Geophysical Research (Space Physics) 111(A10), 10
Xu, Y., Cao, W., Liu, C., Yang, G., Qiu, J., Jing, J., Denker, C., & Wang, H.: 2004, Ap. J. Lett. 607, L131
Yashiro, S., Gopalswamy, N., Akiyama, S., Michalek, G., & Howard, R. A.: 2005, Journal of Geophysical Research (Space Physics) 110, 12
Yokoyama, T., Akita, K., Morimoto, T., Inoue, K., & Newmark, J.: 2001, Ap. J. Lett. 546, L69
Zarro, D. M., Sterling, A. C., Thompson, B. J., Hudson, H. S., & Nitta, N.: 1999, Ap. J. Lett. 520, L139
Zhang, J., Dere, K. P., Howard, R. A., & Vourlidas, A.: 2004, Ap. J. 604, 420
Zirin, H. & Liggett, M. A.: 1987, Solar Phys. 113, 267

Index